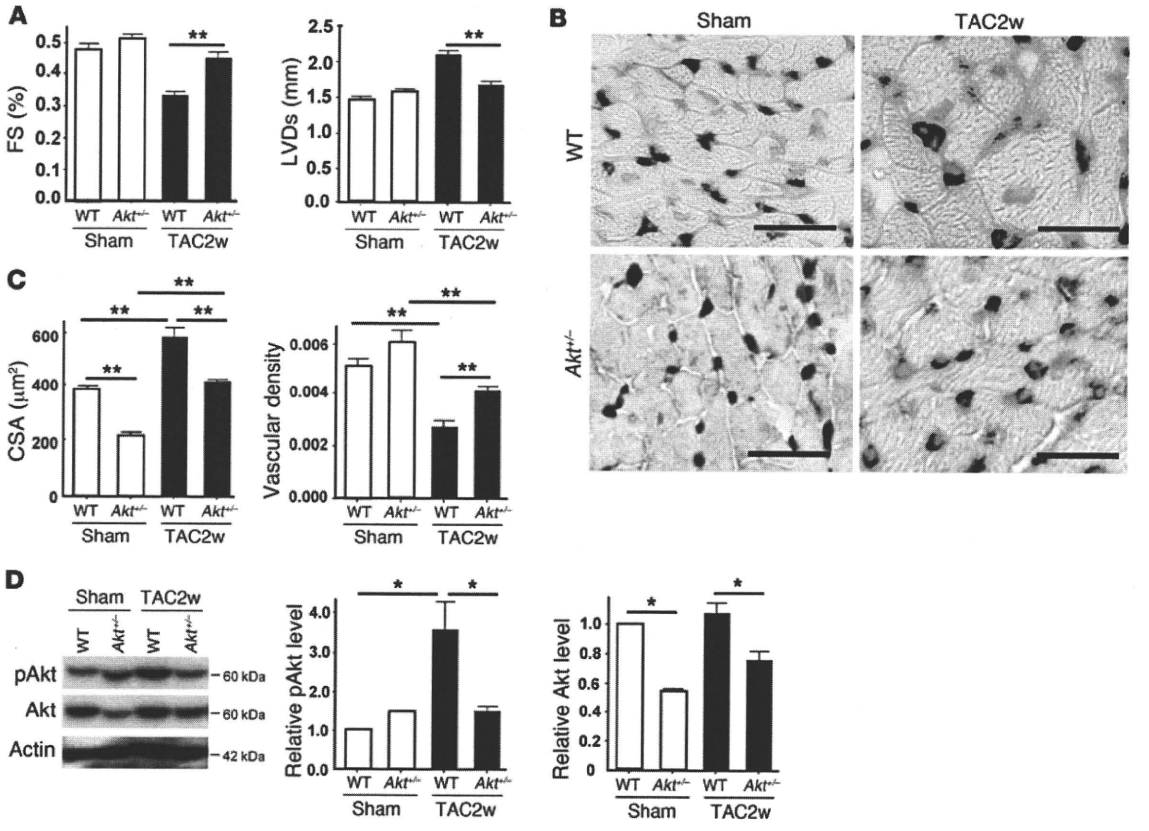

Figure 6

Reduced activation of Akt attenuates systolic dysfunction due to pressure overload. (**A**) *Akt1*-deficient (*Akt1*$^{+/-}$) mice and WT littermates were subjected to TAC or sham operation. Cardiac hypertrophy and systolic function were assessed by echocardiography at 2 weeks after operation. $n = 4$–6. (**B**) Immunohistochemistry using antibodies against platelet and endothelial cell adhesion molecules (dark brown) and dystrophin (light brown) was performed at 2 weeks after operation. Scale bars: 20 μm. (**C**) CSA of cardiomyocytes and relative vascular density were estimated as described in Methods. $n = 3$. (**D**) pAkt and Akt levels in the heart at 2 weeks after operation were examined by Western blot analysis. Graphs indicate relative expression levels of pAkt and Akt. $n = 3$. Data are shown as mean ± SEM. $^*P < 0.05$; $^{**}P < 0.01$.

myocardial metabolism that are characterized by a decrease of FA metabolism and an increase of myocardial glucose metabolism, a pattern similar to that shown in animal models of HF (33). Under these conditions, increased FA metabolism in the heart is pathogenic and the extent of abnormal FA metabolism predicts both morphologic changes of the heart and a poor clinical outcome (34). In this respect, activation of the insulin/Akt pathway in the failing heart appears to be an adaptive response, but constitutive activation of this pathway also leads to activation of growth signals that results in dysregulated hypertrophy, cardiac hypoxia, and systolic dysfunction. Thus, a metabolic modulator that increases glucose uptake (or decreases FA metabolism) without activation of insulin signaling would be a better strategy for the treatment of HF because these patients have systemic insulin resistance. Our results also suggest that the use of insulin to control hyperglycemia can be harmful, especially in the setting of pressure overload, a finding that is consistent with the outcome of a recent clinical trial (16).

Multiple counterregulatory hormones and cytokines are upregulated in HF and are likely to play a role in insulin resistance and altered glucose disposition (21). Upregulation of catecholamines not only contributes directly to the pathogenesis of cardiomyopathy but also increases insulin resistance and thereby indirectly affects systolic function. We also found that chronic pressure overload increased the production of proinflammatory cytokines by adipose tissue, thus promoting systemic insulin resistance (I. Shimizu and T. Minamino, unpublished observations). Further investigation of the link between insulin resistance and HF will continue to provide novel insights into the treatment of HF.

Methods

Animal models. All animal study protocols were approved by the Chiba University Review Board. C57BL/6 mice were purchased from SLC Japan. TAC was performed as described previously (15) in 11-week-old male mice. Sham-operated mice underwent the same procedure except for aortic constriction. For the type 1 diabetic model, 7-week-old male C57BL/6 mice were treated with i.p. STZ in 0.1 M sodium citrate (pH 4.5) at a dose of 50 mg/kg for 5 days. TAC was performed 4 weeks after STZ treatment. In the insulin-treated group, mice received daily i.p. injection of insulin (0.1 IU/g/d) from 9 weeks (2 weeks after STZ treatment) to 13 weeks of age (2 weeks after TAC). In some experiments, mice received an i.p. injection of insulin (1 IU/kg) 30 minutes before sacrifice to investigate the insulin sensitivity of various organs. *Akt1*-deficient mice (*Akt1*$^{+/-}$) were a gift from Morris J. Birnbaum (University of Pennsylvania School of Medicine, Philadelphia, Pennsylvania, USA). The generation and genotyping of *Akt1*-deficient mice, floxed *Insr* mice, and MHC-Cre mice have been described previously (18, 19, 35). Littermate controls have the genotype *Insr*$^{flox/+}$ or *Insr*$^{flox/flox}$. We

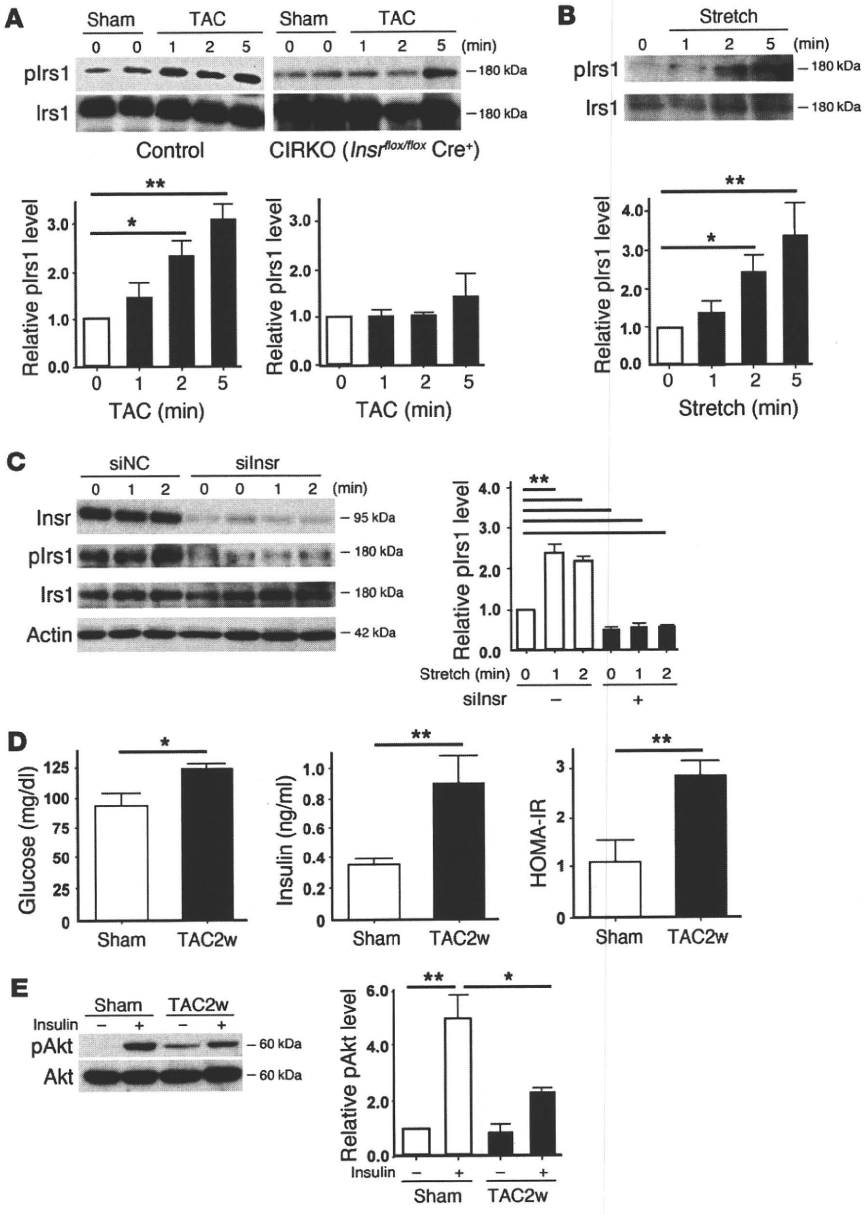

Figure 7

Mechanism of enhanced insulin signaling in the heart during pressure overload. (**A**) CIRKO mice (*Insr*$^{flox/flox}$Cre^{+}) or littermate controls were subjected to TAC or sham operation, and heart samples were obtained at the indicated times. pIrs1 levels were examined by Western blot analysis. The graphs indicate relative expression levels of pIrs1. $n = 3$. (**B**) Cardiomyocytes were subjected to mechanical stretch and pIrs1 levels were examined by Western blot analysis. $n = 3$. (**C**) siRNA targeting Insr (siInsr) or negative control RNA (siNC) was introduced into cardiomyocytes, after which the cells were subjected to mechanical stretch. pIrs1 levels were examined by Western blot analysis. $n = 3$. (**D**) Plasma glucose and insulin levels were examined at 2 weeks after TAC. $n = 7$–8. (**E**) Insulin-induced phosphorylation of Akt (pAkt) in the liver was examined after TAC or sham operation. $n = 3$. Data are shown as mean ± SEM. $^{*}P < 0.05$; $^{**}P < 0.01$.

administered adenoviral vector encoding COMP-Ang1 to mice i.v. after TAC operation as previously described (17).

Physiological and histological analyses. Echocardiography was performed with a Vevo 770 High Resolution Imaging System (Visual Sonics Inc.). To minimize variation of the data, the heart rate was always approximately 500–600 beats per minute when cardiac function was assessed. Cardiac tissue was fixed by perfusion with 4% paraformaldehyde. The fixed sample was immersed in OCT compounds (Miles Inc.) and snap-frozen in liquid nitrogen to prepare cryostat sections. Frozen cross sections of hearts were immunohistochemically double stained with antibodies for PECAM (BD Biosciences – Pharmingen) and dystrophin (Novocastra Laboratories). For measurement of the CSA of cardiomyocytes, 50 randomly selected cardiomyocytes in a left ventricular cross section were measured by tracing dystrophin immunostaining with NIH ImageJ software (http://rsbweb.nih.gov/ij/). Using the same sections, the number of PECAM-positive vessels was counted, and vascular density was estimated as the number of microvessels/number of cardiomyocytes/CSA. Tissue hypoxia was estimated with the Hypoxyprobe-1 (Chemicon) according to the manufacturer's instructions. Briefly, an i.p. injection of pimonidazole (60 mg/kg) was performed 90 minutes before sacrifice. Heart samples were harvested and fixed in 10% formalin overnight. The samples were embedded in paraffin, sectioned at 4-μm thickness, and stained with the Hypoxyprobe-1 monoclonal antibody (clone 4.3.11.3), which binds to protein adducts of pimonidazole in hypoxic cells. TUNEL labeling was performed according to the manufacturer's protocol (In Situ Apoptosis Detection Kit; TaKaRa) in combination with immunostaining for appropriate cell markers.

Western blot analysis. Whole-cell lysates were prepared in lysis buffer (10 mM Tris-HCl, pH 8, 140 mM NaCl, 5 mM EDTA, 0.025% NaN3, 1% Triton X-100, 1% deoxycholate, 0.1% SDS, 1 mM PMSF, 5 μg/ml leupeptin, 2 μg/ml aprotinin, 50 mM NaF, and 1 mM Na_2VO_3). The lysates (40–50 μg) were resolved by SDS-PAGE. Proteins were transferred to a PVDF membrane (Millipore), which was incubated with the primary antibody followed by anti-rabbit or anti-mouse immunoglobulin-G conjugated with horseradish peroxidase (Jackson). Specific proteins were detected by enhanced chemiluminescence

(Amersham). The primary antibodies used for Western blotting were as follows: anti-pIrs1 antibody (Tyr612, Biomol), anti-Irs1 antibody (C20), anti-Akt1 antibody (C20), anti-Insr β antibody (C-19) (Santa Cruz Biotechnology Inc.), anti-phospho-Akt antibody (Ser473), anti-phospho-p44/42 MAP kinase antibody (Thr202/Tyr204), anti-MAP kinase (ERK1+ERK2) antibody (Invitrogen), and anti-actin antibody (Sigma-Aldrich). Plasma insulin levels were evaluated with an ELISA kit (Morinaga Institute of Biological Science Inc.) according to the manufacturer's instructions.

Cell culture. Neonatal Wistar rats were purchased from Takasugi Experimental Animal Supply. Cardiomyocytes were prepared from neonatal rats and cultured as described previously (15). Passive stretching of cultured cells was done as described previously. Cells were plated on collagen-coated silicone rubber dishes (STREX Mechanical Cell Strain Instruments), and the silicone dishes were stretched by attaching both ends of each dish firmly to a fixed frame, resulting in longitudinal stretch by 20% of the original length. siRNA targeting Insr, IGF, and the IGF-1 receptor was purchased from Invitrogen and introduced into rat cardiomyocytes by using Lipofectamine RNAiMax (Invitrogen) according to the manufacturer's instructions.

Statistics. Data are shown as the mean ± SEM. Differences between groups were examined by 2-tailed Student's *t* test or ANOVA, followed by Bonferroni's correction for comparison of means. For all analyses, $P < 0.05$ was considered statistically significant.

Acknowledgments

We thank Morris J. Birnbaum for *Akt1*-deficient mice. This work was supported by a Grant-in-Aid for Scientific Research from the Ministry of Education, Science, Sports, and Culture and Health and Labor Sciences research grants (to I. Komuro); a Grant-in-Aid for Scientific Research from the Ministry of Education, Culture, Sports, Science and Technology of Japan; and grants from the Suzuken Memorial Foundation; the Japan Diabetes Foundation; the Ichiro Kanehara Foundation; the Tokyo Biochemical Research Foundation; the Takeda Science Foundation; the Cell Science Research Foundation; the Japan Foundation of Applied Enzymology; and the Astellas Foundation for Research on Metabolic Disorders (to T. Minamino).

Received for publication June 5, 2009, and accepted in revised form February 10, 2010.

Address correspondence to: Issei Komuro, Department of Cardiovascular Science and Medicine, Chiba University Graduate School of Medicine, 1-8-1 Inohana, Chuo-ku, Chiba 260-8670, Japan. Phone: 81.43.226.2097; Fax: 81.43.226.2557; E-mail: komuro-tky@umin.ac.jp.

1. Frey N, Olson EN. Cardiac hypertrophy: the good, the bad, and the ugly. *Annu Rev Physiol.* 2003;65:45–79.
2. Adams TD, Yanowitz FG, Fisher AG, Ridges JD, Lovell K, Pryor TA. Noninvasive evaluation of exercise training in college-age men. *Circulation.* 1981; 64(5):958–965.
3. Pelliccia A, Maron BJ. Outer limits of the athlete's heart, the effect of gender, and relevance to the differential diagnosis with primary cardiac diseases. *Cardiol Clin.* 1997;15(3):381–396.
4. Heineke J, Molkentin JD. Regulation of cardiac hyperrtrophy by intracellular signalling pathways. *Nat Rev Mol Cell Biol.* 2006;7(8):589–600.
5. Belke DD, et al. Insulin signaling coordinately regulates cardiac size, metabolism, and contractile protein isoform expression. *J Clin Invest.* 2002; 109(5):629–639.
6. Hu P, Zhang D, Swenson L, Chakrabarti G, Abel ED, Litwin SE. Minimally invasive aortic banding in mice: effects of altered cardiomyocyte insulin signaling during pressure overload. *Am J Physiol Heart Circ Physiol.* 2003;285(3):H1261–H1269.
7. Shioi T, et al. The conserved phosphoinositide 3-kinase pathway determines heart size in mice. *EMBO J.* 2000;19(11):2537–2548.
8. McMullen JR, et al. Phosphoinositide 3-kinase (p110α) plays a critical role for the induction of physiological, but not pathological, cardiac hypertrophy. *Proc Natl Acad Sci U S A.* 2003;100(21):12355–12360.
9. DeBosch B, et al. Akt1 is required for physiological cardiac growth. *Circulation.* 2006;113(17):2097–2104.
10. Samuelsson AM, et al. Hyperinsulinemia: effect on cardiac mass/function, angiotensin II receptor expression, and insulin signaling pathways. *Am J Physiol Heart Circ Physiol.* 2006;291(2):H787–H796.
11. Condorelli G, et al. Akt induces enhanced myocardial contractility and cell size in vivo in transgenic mice. *Proc Natl Acad Sci U S A.* 2002;99(19):12333–12338.
12. Matsui T, et al. Phenotypic spectrum caused by transgenic overexpression of activated Akt in the heart. *J Biol Chem.* 2002;277(25):22896–22901.
13. Shioi T, et al. Akt/protein kinase B promotes organ growth in transgenic mice. *Mol Cell Biol.* 2002; 22(8):2799–2809.
14. Shiojima I, et al. Disruption of coordinated cardiac hypertrophy and angiogenesis contributes to the transition to heart failure. *J Clin Invest.* 2005; 115(8):2108–2118.
15. Sano M, et al. p53-induced inhibition of Hif-1 causes cardiac dysfunction during pressure overload. *Nature.* 2007;446(7134):444–448.
16. Gerstein HC, et al. Effects of intensive glucose lowering in type 2 diabetes. *N Engl J Med.* 2008; 358(24):2545–2559.
17. Cho CH, et al. Long-term and sustained COMP-Ang1 induces long-lasting vascular enlargement and enhanced blood flow. *Circ Res.* 2005;97(1):86–94.
18. Abel ED, et al. Cardiac hypertrophy with preserved contractile function after selective deletion of GLUT4 from the heart. *J Clin Invest.* 1999;104(12):1703–1714.
19. Bruning JC, et al. A muscle-specific insulin receptor knockout exhibits features of the metabolic syndrome of NIDDM without altering glucose tolerance. *Mol Cell.* 1998;2(5):559–569.
20. Zou Y, et al. Mechanical stress activates angiotensin II type 1 receptor without the involvement of angiotensin II. *Nat Cell Biol.* 2004;6(6):499–506.
21. Witteles RM, Fowler MB. Insulin-resistant cardiomyopathy clinical evidence, mechanisms, and treatment options. *J Am Coll Cardiol.* 2008;51(2):93–102.
22. Sharma N, Okere IC, Duda MK, Chess DJ, O'Shea KM, Stanley WC. Potential impact of carbohydrate and fat intake on pathological left ventricular hypertrophy. *Cardiovasc Res.* 2007;73(2):257–268.
23. Swan JW, et al. Insulin resistance in chronic heart failure: relation to severity and etiology of heart failure. *J Am Coll Cardiol.* 1997;30(2):527–532.
24. Ingelsson E, Sundstrom J, Arnlov J, Zethelius B, Lind L. Insulin resistance and risk of congestive heart failure. *JAMA.* 2005;294(3):334–341.
25. Arnlov J, et al. Several factors associated with the insulin resistance syndrome are predictors of left ventricular systolic dysfunction in a male population after 20 years of follow-up. *Am Heart J.* 2001; 142(4):720–724.
26. Hasegawa S, Kusuoka H, Maruyama K, Nishimura T, Hori M, Hatazawa J. Myocardial positron emission computed tomographic images obtained with fluorine-18 fluoro-2-deoxyglucose predict the response of idiopathic dilated cardiomyopathy patients to beta-blockers. *J Am Coll Cardiol.* 2004; 43(2):224–233.
27. Garcia-Puig J, Ruilope LM, Luque M, Fernandez J, Ortega R, Dal-Re R. Glucose metabolism in patients with essential hypertension. *Am J Med.* 2006; 119(4):318–326.
28. Karason K, Sjostrom L, Wallentin I, Peltonen M. Impact of blood pressure and insulin on the relationship between body fat and left ventricular structure. *Eur Heart J.* 2003;24(16):1500–1505.
29. Brutsaert DL. Cardiac endothelial-myocardial signaling: its role in cardiac growth, contractile performance, and rhythmicity. *Physiol Rev.* 2003;83(1):59–115.
30. Neubauer S. The failing heart--an engine out of fuel. *N Engl J Med.* 2007;356(11):1140–1151.
31. Christe ME, Rodgers RL. Altered glucose and fatty acid oxidation in hearts of the spontaneously hypertensive rat. *J Mol Cell Cardiol.* 1994;26(10):1371–1375.
32. Barger PM, Kelly DP. Fatty acid utilization in the hypertrophied and failing heart: molecular regulatory mechanisms. *Am J Med Sci.* 1999;318(1):36–42.
33. Davila-Roman VG, et al. Altered myocardial fatty acid and glucose metabolism in idiopathic dilated cardiomyopathy. *J Am Coll Cardiol.* 2002;40(2):271–277.
34. Yazaki Y, et al. Assessment of myocardial fatty acid metabolic abnormalities in patients with idiopathic dilated cardiomyopathy using 123I BMIPP SPECT: correlation with clinicopathological findings and clinical course. *Heart.* 1999;81(2):153–159.
35. Cho H, Thorvaldsen JL, Chu Q, Feng F, Birnbaum MJ. Akt1/PKBalpha is required for normal growth but dispensable for maintenance of glucose homeostasis in mice. *J Biol Chem.* 2001;276(42):38349–38352.

Promotion of CHIP-Mediated p53 Degradation Protects the Heart From Ischemic Injury

Atsuhiko T. Naito, Sho Okada, Tohru Minamino, Koji Iwanaga, Mei-Lan Liu, Tomokazu Sumida, Seitaro Nomura, Naruhiko Sahara, Tatsuya Mizoroki, Akihiko Takashima, Hiroshi Akazawa, Toshio Nagai, Ichiro Shiojima, Issei Komuro

Rationale: The number of patients with coronary heart disease, including myocardial infarction, is increasing and novel therapeutic strategy is awaited. Tumor suppressor protein p53 accumulates in the myocardium after myocardial infarction, causes apoptosis of cardiomyocytes, and plays an important role in the progression into heart failure.

Objectives: We investigated the molecular mechanisms of p53 accumulation in the heart after myocardial infarction and tested whether anti-p53 approach would be effective against myocardial infarction.

Methods and Results: Through expression screening, we found that CHIP (carboxyl terminus of Hsp70-interacting protein) is an endogenous p53 antagonist in the heart. CHIP suppressed p53 level by ubiquitinating and inducing proteasomal degradation. CHIP transcription was downregulated after hypoxic stress and restoration of CHIP protein level prevented p53 accumulation after hypoxic stress. CHIP overexpression in vivo prevented p53 accumulation and cardiomyocyte apoptosis after myocardial infarction. Promotion of CHIP function by heat shock protein (Hsp)90 inhibitor, 17-allylamino-17-demethoxy geldanamycin (17-AAG), also prevented p53 accumulation and cardiomyocyte apoptosis both in vitro and in vivo. CHIP-mediated p53 degradation was at least one of the cardioprotective effects of 17-AAG.

Conclusions: We found that downregulation of CHIP level by hypoxia was responsible for p53 accumulation in the heart after myocardial infarction. Decreasing the amount of p53 prevented myocardial apoptosis and ameliorated ventricular remodeling after myocardial infarction. We conclude that anti-p53 approach would be effective to treat myocardial infarction. (*Circ Res.* 2010;106:1692-1702.)

Key Words: myocardial infarction ■ CHIP ■ p53 ■ hypoxia

The number of patients with coronary heart disease has been increasing and cardiovascular diseases are the leading cause of deaths in the Western world. Despite the development of pharmacological and nonpharmacological interventions, 33% of the men and 43% of the women die within 5 years after myocardial infarction (MI).[1] Therefore, a novel therapeutic approach against coronary heart disease is awaited.

Apoptosis of cardiomyocytes is accompanied with acute coronary occlusion.[2] Because apoptotic loss of cardiomyocytes causes heart failure,[3] inhibition of apoptosis has been suggested as an additional therapeutic approach to coronary heart disease.[4] In mice, overexpression of antiapoptotic Bcl-2 protein or genetic deletion of proapoptotic Bax protein have been reported to prevent apoptosis and reduce infarct size,[5–8] implicating that antiapoptotic approach is effective for prevention of ventricular remodeling after myocardial infarction.

The tumor suppressor *p53* is an important transcription factor that regulates cell cycle progression, cellular senescence, and apoptosis. Under physiological condition, p53 protein level is maintained low, but is elevated when cells are stressed or damaged.[9] The mechanism for keeping p53 protein level low involves several E3 ubiquitin ligases such as MDM2,[10,11] COP1,[12] and Pirh2.[13] Importantly, the expression of these proteins were positively regulated by p53, suggesting the role for negative-feedback loop against p53 elevation.

Protein level of p53 is also kept low in the heart but it is elevated when cardiac cells are exposed to hypoxia.[14–16]

Original received December 4, 2009; revision received April 6, 2010; accepted April 12, 2010.

From the Department of Cardiovascular Science and Medicine (A.T.N., S.O., T. Minamino, K.I., M.-L.L., T.S., S.N., H.A., T.N., I.S., I.K.), Chiba University Graduate School of Medicine, Japan; Department of Cardiovascular Medicine (A.T.N., H.A., I.S., I.K.), Osaka University Graduate School of Medicine, Japan; PRESTO (T. Minamino), Japan Science and Technology Agency, Saitama, Japan; and Laboratory for Alzheimer's Disease (N.S., T. Mizoroki, A.T.). RIKEN Brain Science Institute, Saitama, Japan.

This manuscript was sent to Junichi Sadoshima, Consulting Editor, for review by expert referees, editorial decision, and final disposition.

Correspondence to Issei Komuro, MD, PhD, Department of Cardiovascular Science and Medicine, Chiba University Graduate School of Medicine, 1-8-1 Inohana, Chuo-ku, Chiba, Japan. E-mail komuro-tky@umin.ac.jp

Circulation Research is available at http://circres.ahajournals.org DOI: 10.1161/CIRCRESAHA.109.214346

We have recently reported that elevation of p53 causes the development of pressure overload-induced heart failure.[16] We have also observed the elevation of p53 protein levels after myocardial infarction and shown that *p53* gene deletion improved cardiac function after myocardial infarction,[16] suggesting that the inhibition of p53 might become a novel therapeutic strategy for ischemic heart diseases.

As an initial approach for the investigation of anti-p53 therapy, we searched for an endogenous p53 antagonist in the heart. Through expression screening, we found that CHIP (carboxyl terminus of Hsp70-interacting protein) is an endogenous p53 antagonist that keeps p53 level low in the heart. We also found that CHIP downregulation is involved in the mechanism of p53 accumulation in the heart after myocardial infarction. Facilitating CHIP-mediated p53 degradation prevented apoptosis of cardiomyocytes and ameliorated ventricular remodeling in the postinfarct heart. The present study revealed the mechanism of p53 accumulation in the heart after myocardial ischemia and suggested that anti-p53 approach would be effective to treat myocardial infarction.

Non-standard Abbreviations and Acronyms

17-AAG	17-allylamino-17-demethoxy geldanamycin
CHIP	carboxyl terminus of Hsp70-interacting protein
HIF	hypoxia-inducible factor
HRE	hypoxia-responsive element
Hsp	heat shock protein
HW/BW	heart weight/body weight
MI	myocardial infarction
PARP	poly(ADP-ribose)polymerase
siRNA	small interfering RNA

Methods

Expression Cloning

Expression cloning was performed as described previously[17] using PG13-Luc (kind gift from B. Vogelstein, Ludwig Center for Cancer Genetics and Therapeutics, Howard Hughes Medical Institute, and Sidney Kimmel Cancer Center, Johns Hopkins Medical Institutions, Baltimore, Md) as a reporter plasmid. Initially, cDNA expression library from human heart (Invitrogen) was separated into small pools that contain ≈100 clones each. cDNA clones that downregulate PG13 activity were isolated by sib-selection.

Cell Culture

COS7 and HEK293 cells are from ATCC and cultured in DMEM containing 10% FBS (Invitrogen). Neonatal rat cardiomyocytes were isolated from 1-day-old Wistar rats and cultured as described previously.[18] Cardiomyocytes were exposed to hypoxic stress by culturing under $CoCl_2$ or by culturing in hypoxic chamber (<1% O_2; Po_2, 18 to ≈20 mm Hg).

Animals

All protocols were approved by Chiba University review board. CHIP knockout mice and cardiac-specific inducible hypoxia-inducible factor (HIF)-1 knockout mice were described.[16,19,20] Heterozygous CHIP knockout mice were used in this study because homozygous knockout mice were perinatally lethal.[20] Cardiac-specific CHIP transgenic mice were generated by pronuclear injection of αMHC-HA-CHIP transgene construct. Coronary artery ligation was performed on 10-week old male mice as described previously.[21]

Statistical Analysis

Data are expressed as means±SE. The significance of differences among means was evaluated using analysis of variance (ANOVA), followed by Fisher's protected least significant difference test and Dunnett's test for multiple comparisons. Significant differences were defined as $P<0.05$.

Results

Identification of CHIP As a Novel p53 Antagonist From Heart cDNA Library

To elucidate novel p53 antagonists in the heart, we performed expression screening by expressing cDNA pools in COS7 cells together with a reporter plasmid, PG13-luciferase, which contains 13 copies of p53 binding site upstream of luciferase gene and responsive to wild-type p53 dependent transcription. From the screening of 500 cDNA pools, each containing around 100 individual cDNA clones obtained from human heart cDNA library, we found 5 pools that suppress the PG13 activity. Individual cDNA clone that downregulates the PG13 activity was identified by sib-selection. One of the molecules that was highly expressed in the heart (Figure I, A, in the Online Data Supplement, available at http://circres.ahajournals.org) was CHIP (also called STUB1 [Stip1 homology and U-box containing protein]), a chaperone-interacting protein with E3 ubiquitin ligase activity.[22] Transfection of CHIP suppressed endogenous and exogenous (by overexpression of p53) PG13 activity (Figure 1A) and decreased the protein levels of p53 (Figure 1B) in a plasmid dose-dependent manner in COS7 cells. Direct interaction between CHIP and p53 was confirmed both at the exogenous level in COS7 cells (Online Figure I, B) and at the endogenous level in cardiomyocytes (Online Figure I, C). Western blotting using anti-ubiquitin antibody after immunoprecipitation with p53 revealed that overexpression of CHIP increased poly-ubiquitinated p53 (which appears as a smear) (Online Figure I, D). The proteasomal inhibitor MG132 restored p53 protein level that was suppressed by CHIP (Online Figure I, E), indicating that CHIP directs p53 for proteasome-mediated degradation. When CHIP was knocked down in cardiomyocytes using small interfering (si)RNA, p53 expression was upregulated (Figure 1C), and p53 protein levels following CHIP knockdown were comparable to those induced by the knockdown of MDM2, a well known E3 ubiquitin ligase for p53 (Figure 1D). CHIP protein level was not changed by knockdown of MDM2 (Figure 1D). p53 protein levels were also markedly elevated in the heart of CHIP heterozygous mice (Figure 1E). These results suggest that CHIP induces degradation of wild-type p53 protein in cardiomyocytes, which is consistent with previous reports in other cells (H1299 cells and U2OS cells).[23,24] In addition, we revealed that CHIP is a crucial negative regulator that keeps p53 protein levels low in the heart under physiological conditions.

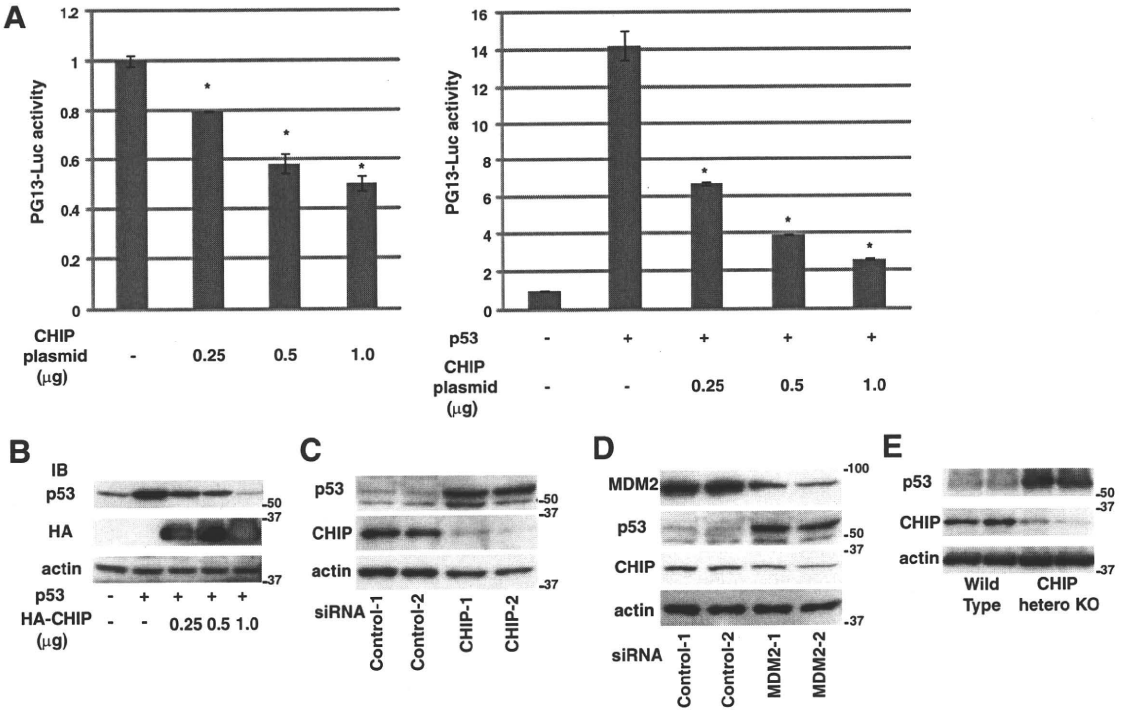

Figure 1. CHIP is a crucial negative regulator of p53 expression in the heart. A, Transfection of CHIP expressing plasmid suppressed endogenous **(left)** and exogenous **(right)** p53 transcriptional activity. *$P<0.01$ vs control; n=5. **B,** CHIP decreases p53 protein levels in COS7 cells. IB indicates immunoblot. **C,** p53 expression is upregulated by CHIP knockdown in cardiomyocytes. siRNAs specific to CHIP (CHIP-1 and CHIP-2), or control siRNA were transfected into cultured cardiomyocytes and protein levels of CHIP and p53 were examined by Western blotting. CHIP-1 and CHIP-2 represent 2 different siRNAs against CHIP. Control-1 is a commercially available control RNA, and control-2 is a scrambled control RNA. **D,** p53 upregulation is also observed by MDM2 knockdown. siRNAs specific to MDM2 (MDM2–1 and MDM2–2) or control siRNA were transfected into cultured cardiomyocytes, and protein levels of CHIP, p53, and MDM2 were examined by Western blotting. The extent of p53 upregulation by MDM2 knockdown was comparable to that induced by CHIP knockdown. **E,** Total protein of wild-type and CHIP heterozygous mice were analyzed by Western blotting. p53 expression is upregulated in the heart of CHIP heterozygous mice.

Molecular Mechanisms of Hypoxia-Induced p53 Accumulation

As CHIP regulates p53 status in the heart, we speculated that CHIP might be involved in the molecular mechanism of hypoxia-induced p53 accumulation in the heart. Cobalt chloride ($CoCl_2$) increases HIF-1 activity through preventing HIF-1α protein degradation and is widely used as a hypoxia mimicking reagent.[25,26] Treatment of cardiomyocytes with $CoCl_2$ (250 μmol/L) increased p53 protein level with a marked downregulation of CHIP protein level (Figure 2A). Notably, the expression of MDM2 was rather increased in this experimental condition. Because transcriptional regulation of MDM2 is known to be upregulated by p53 as a part of negative-feedback loop, increased MDM2 expression after $CoCl_2$ treatment may possibly be attributable to this feedback system against p53 elevation. Accumulation of p53 and downregulation of CHIP were also observed when cardiomyocytes were cultured in hypoxic chamber for 24 hours (Online Figure I, F). We confirmed that both treatments increased nuclear HIF-1α protein that binds to HIF-1α binding oligonucleotide by commercially available ELISA system (Online Figure I, G). We also analyzed the expression of p53 and CHIP in the heart after MI. p53 protein levels were increased on day 1 after MI and remained upregulated thereafter, whereas expression levels of CHIP were markedly downregulated on day 1, and remained at lower levels than those of controls (Figure 2B and analyzed in Online Figure II, A and B). In contrast, MDM2 protein levels were slightly increased after MI (Figure 2B). The inverse correlation between CHIP and p53 protein level implies the possible involvement of CHIP downregulation in the initiation of p53 accumulation after acute hypoxic stress. Other E3 ubiquitin ligases whose transcription is regulated by p53, such as MDM2, might work to reverse p53 level after initial accumulation of p53 as a feedback system to prevent further detrimental effects that might be elicited by chronic p53 elevation.

To investigate why CHIP is downregulated after hypoxic insult, we tested whether HIF-1 mediates hypoxia-induced downregulation of CHIP, because HIF-1 is known to downregulate some of its target genes through hypoxia-responsive element (HRE).[27–30] Human CHIP promoter (from −329 bases upstream of transcription start site to +39 bases downstream of transcription start site) that contains a conserved HRE at −49 (Figure 2C) was cloned upstream of luciferase reporter gene (pGL4-CHIP). pGL4-CHIP activity was significantly suppressed by both $CoCl_2$ treatment (24 hours) and HIF-1α overexpression in COS7 cells (Figure 2D). When a mutation was introduced into HRE at −49 (pGL4-CHIP-mutHRE), the luciferase activity was no longer responsive to hypoxic stress or HIF-1α overexpression (Figure 2D), suggesting that *CHIP* gene expression is downregu-

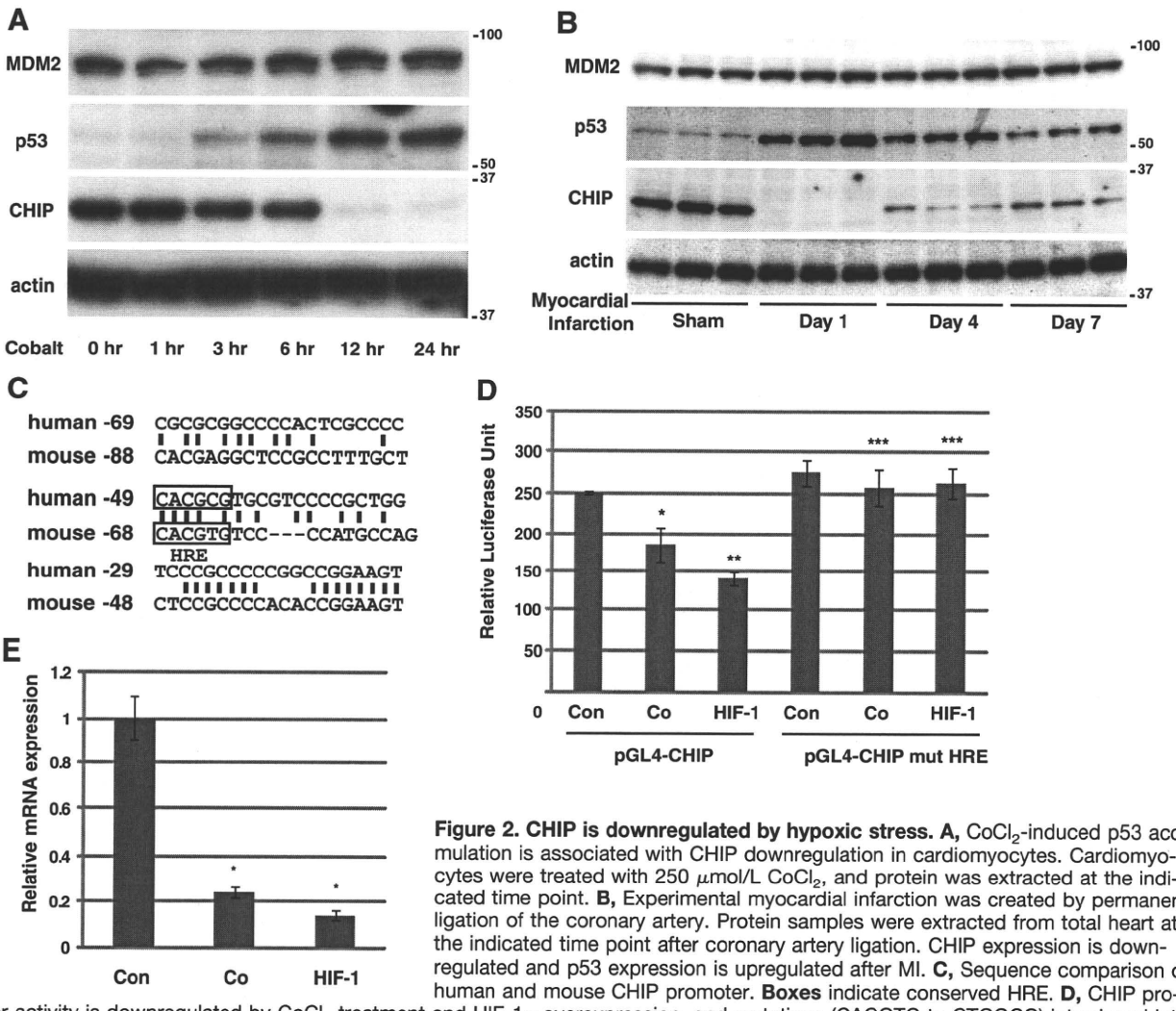

Figure 2. CHIP is downregulated by hypoxic stress. A, $CoCl_2$-induced p53 accumulation is associated with CHIP downregulation in cardiomyocytes. Cardiomyocytes were treated with 250 μmol/L $CoCl_2$, and protein was extracted at the indicated time point. **B,** Experimental myocardial infarction was created by permanent ligation of the coronary artery. Protein samples were extracted from total heart at the indicated time point after coronary artery ligation. CHIP expression is downregulated and p53 expression is upregulated after MI. **C,** Sequence comparison of human and mouse CHIP promoter. **Boxes** indicate conserved HRE. **D,** CHIP promoter activity is downregulated by $CoCl_2$ treatment and HIF-1α overexpression, and mutations (CACGTG to CTGGCG) introduced into HRE at −49 abrogated this response. CHIP promoter sequence from human genomic DNA (−329 to +39 from transcription start site) was cloned upstream of luciferase gene. Mutation was introduced using a kit from Stratagene. Luciferase assay was performed 24 hours after $CoCl_2$ treatment or HIF-1α overexpression. *$P<0.05$, **$P<0.01$, ***P=NS vs control; n=5. **E,** Real-time PCR analysis revealed mRNA level of CHIP was also downregulated by hypoxic stress (Co) and HIF-1α overexpression. RNA was extracted 24 hours after $CoCl_2$ treatment or HIF-1α overexpression. *$P<0.01$.

lated by HIF-1 at the transcriptional level through HRE. Real-time PCR analysis revealed that exposure of cardiomyocytes to $CoCl_2$ (24 hours) and adenoviral overexpression of constitutively active HIF-1α led to marked downregulation of CHIP mRNA levels (Figure 2E), further supporting our data that hypoxic stress downregulates CHIP levels. HIF-1α gene is both required and sufficient for hypoxic stress-induced CHIP downregulation and p53 accumulation because knockdown of HIF-1α attenuated the effects of $CoCl_2$ treatment on expressions of p53 and CHIP (Online Figure III, A), and overexpression of constitutively active HIF-1α suppressed CHIP expression and increased p53 expression in cardiomyocytes (Online Figure III, B). Furthermore, downregulation of CHIP protein levels after MI was attenuated in cardiac-specific inducible HIF-1α conditional knockout mice[16] (Online Figure III, C). Collectively, these findings suggest that CHIP transcription is directly downregulated by hypoxia through HIF-1.

CHIP Protects Cardiomyocytes From Hypoxia-Induced p53-Mediated Apoptosis of Cardiomyocytes

Because hypoxia or p53 overexpression induces apoptotic cell death in cultured cardiomyocytes,[14] we next examined whether hypoxia-induced cardiomyocyte apoptosis is mediated by the HIF-1-CHIP-p53 pathway. $CoCl_2$ treatment (24 hours) induced p53 accumulation and promoted apoptosis of cardiomyocytes as assessed by cleaved poly (ADP-ribose) polymerase (PARP) expression (Figure 3A), Annexin V staining (Figure 3B and 3C), and caspase-3 activity (Figure 3D). $CoCl_2$-induced apoptosis was p53-dependent, because knockdown of p53 in $CoCl_2$-treated cardiomyocytes attenuated hypoxia-induced cell death (Figure 3A through 3D). We next assessed whether overexpression of CHIP could rescue $CoCl_2$-induced apoptosis. Adenovirus-mediated overexpression of CHIP in cardiomyocytes markedly downregulated p53 expression and attenuated apoptosis in $CoCl_2$-treated

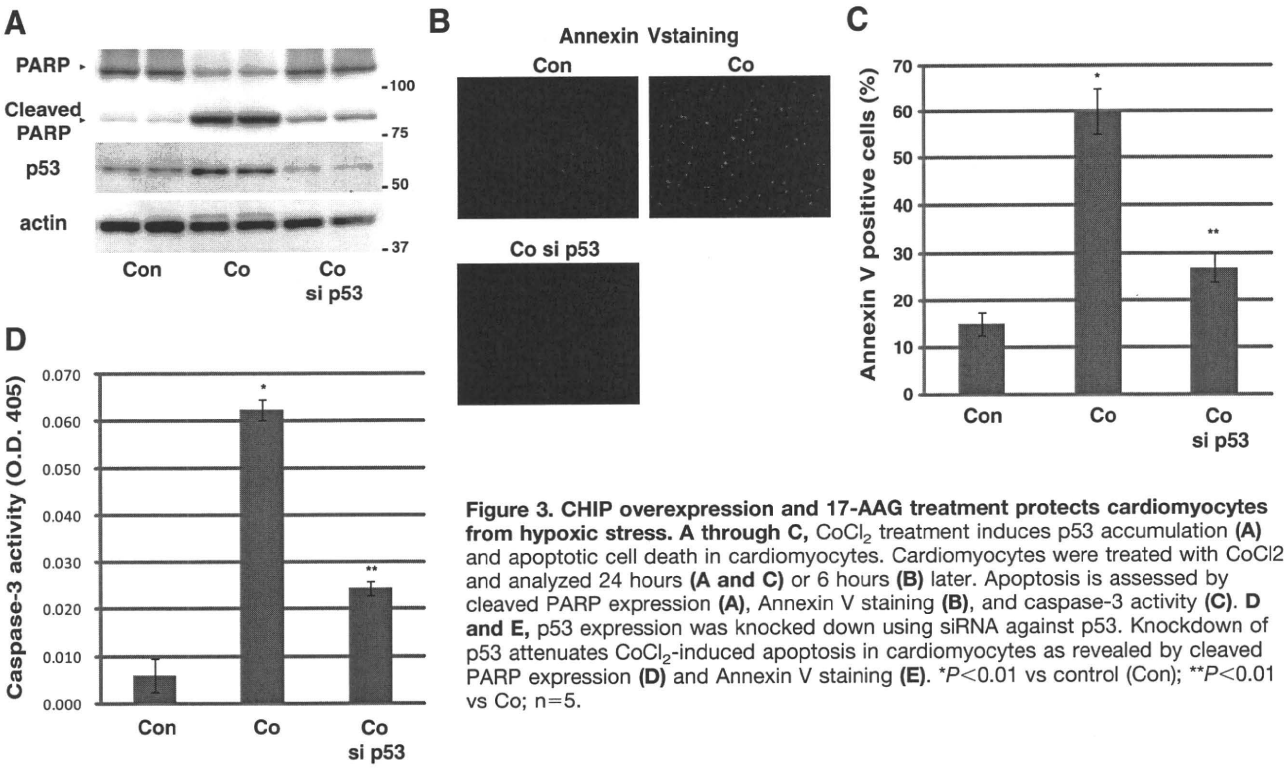

Figure 3. CHIP overexpression and 17-AAG treatment protects cardiomyocytes from hypoxic stress. A through C, $CoCl_2$ treatment induces p53 accumulation **(A)** and apoptotic cell death in cardiomyocytes. Cardiomyocytes were treated with CoCl2 and analyzed 24 hours **(A and C)** or 6 hours **(B)** later. Apoptosis is assessed by cleaved PARP expression **(A)**, Annexin V staining **(B)**, and caspase-3 activity **(C)**. **D and E,** p53 expression was knocked down using siRNA against p53. Knockdown of p53 attenuates $CoCl_2$-induced apoptosis in cardiomyocytes as revealed by cleaved PARP expression **(D)** and Annexin V staining **(E)**. *$P<0.01$ vs control (Con); **$P<0.01$ vs Co; n=5.

cardiomyocytes (Figure 4A through 4C). These results underscore our hypothesis that downregulation of CHIP is responsible for p53 accumulation after hypoxic stress. Moreover, forced expression of CHIP prevented hypoxia-induced cardiomyocyte apoptosis by inducing degradation of p53, suggesting that CHIP-mediated p53 degradation is a potential therapeutic target.

17-AAG Protects Cardiomyocytes From Hypoxia-Induced Apoptosis

Inhibitors for heat shock protein (Hsp)90 have been shown to promote proteasomal degradation of CHIP client proteins and to be effective for the diseases caused by the accumulation of CHIP substrates.[31,32] We therefore examined whether an Hsp90 inhibitor 17-allylamino-17-demethoxy geldanamycin (17-AAG) induces degradation of p53 protein and protects cardiomyocytes from hypoxic stress. In cardiomyocytes treated with $CoCl_2$, 17-AAG downregulated p53 expression (Figure 4D). 17-AAG treatment also suppressed hypoxia-induced cardiomyocyte apoptosis in a CHIP-dependent manner, because CHIP knockdown attenuated the protective effects of 17-AAG (Figure 4E through 4G). These results suggest that 17-AAG protects cardiomyocytes from hypoxic stress by promoting CHIP-mediated p53 degradation.

Interestingly, protein level of CHIP was increased by 17-AAG treatment (Figure 4E). As mRNA level of CHIP was not changed by 17-AAG treatment (Online Figure IV, A), we speculated that protein stability was affected by 17-AAG treatment. When protein translation was inhibited by cycloheximide, 17-AAG treatment dramatically extended the protein half-life of CHIP (Online Figure IV, B and C). 17-AAG also upregulated the protein stability of other proteins, Hsp70 and HSF-1 (Online Figure IV, B and C). Because 17-AAG exerted some antiapoptotic effects even in the cells of negligible CHIP protein level (Figure 4E and 4F), upregulation of these cardioprotective proteins[33,34] might mediate part of the effects of 17-AAG. It remains to be determined how 17-AAG prolongs protein half-life of certain kinds of proteins.

CHIP and 17-AAG Prevent Apoptosis and Ventricular Remodeling After Myocardial Infarction

We next examined whether promotion of CHIP-mediated p53 degradation could attenuate ischemic cardiac injury also in vivo. For this purpose, transgenic mice which overexpress CHIP specifically in the heart (CHIP-Tg) (Figure 5A) were subjected to permanent coronary artery ligation. In CHIP-Tg mice, elevation of p53 protein levels (Figure 5B) and apoptotic cardiomyocyte death in the border zone of the infarct area (Figure 5B and 5C) were attenuated compared to wild-type littermates at 24 hours after the MI operation. Apoptotic death of the cardiomyocytes in the remote zone of the infarct was not changed between littermates (data not shown). We next examined whether this decrease in apoptotic cell death leads to attenuation of cardiac ventricular remodeling. At day 14, CHIP-Tg mice exhibited smaller heart weight/body weight (HW/BW) ratio, better contractility and less ventricular remodeling (Figure 5D and 5E) compared to wild-type littermates. These results provides an evidence for our hypothesis that CHIP downregulation is responsible for p53 accumulation after myocardial infarction, and suggests that CHIP overexpression is protective for the heart by preventing p53 accumulation and cardiomyocyte apoptosis after myocardial infarction.

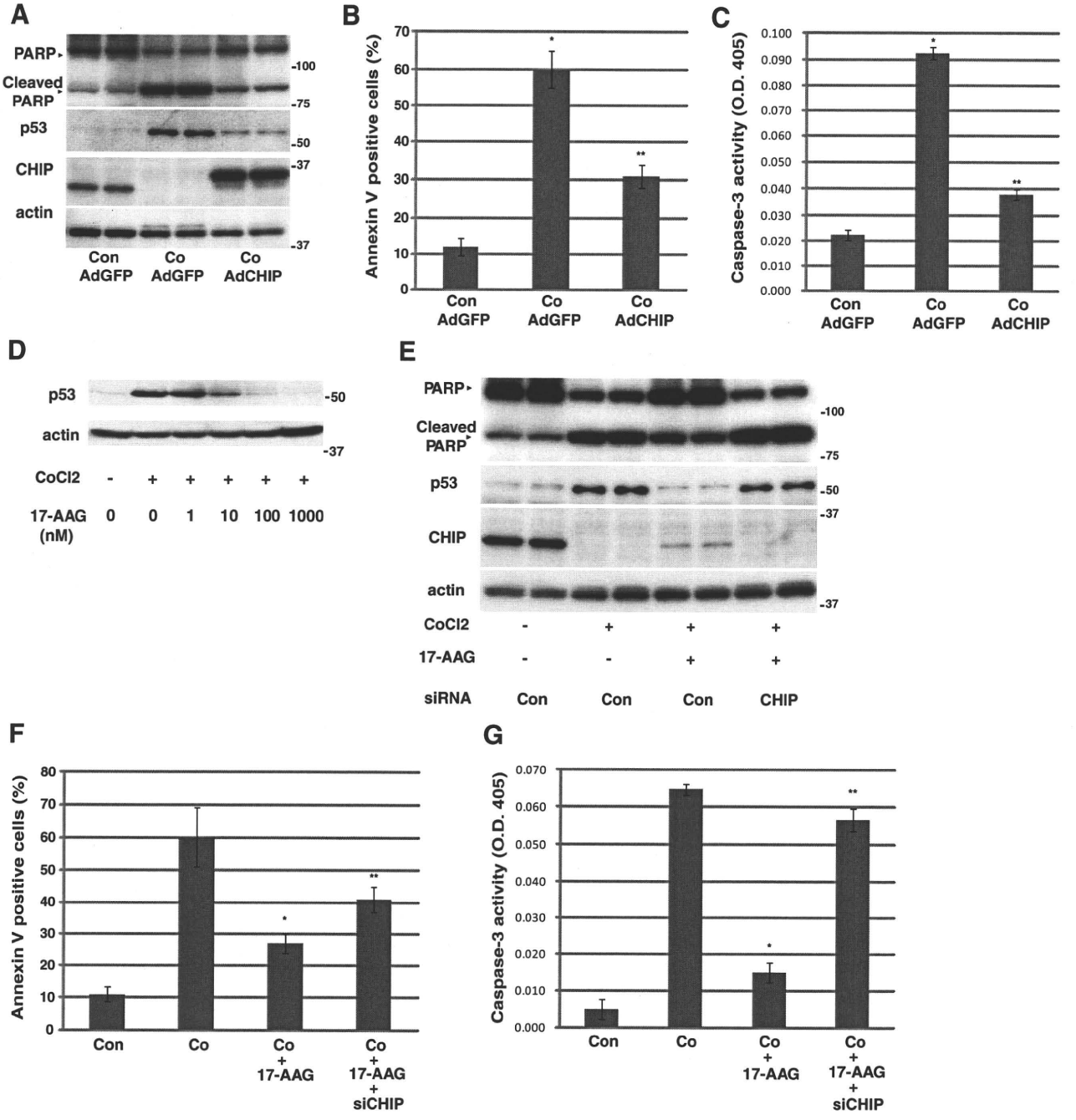

Figure 4. Promoting CHIP-mediated p53 degradation is protective against hypoxic stress. A through C, Overexpression of CHIP attenuates $CoCl_2$-induced p53 accumulation **(A)** and apoptosis in cardiomyocytes. Cardiomyocytes were infected with adenovirus harboring green fluorescent protein (GFP) or CHIP. Twenty-four hours later, culture medium was changed and the cells were treated with $CoCl_2$. Apoptosis was assessed by cleaved PARP expression **(A)**, Annexin V staining **(B)**, and caspase-3 activity **(C)**. *$P<0.01$ vs control (Con)+AdGFP; **$P<0.01$ vs Co+AdGFP; n=5. **D,** 17-AAG downregulates p53 expression in cardiomyocytes. Neonatal rat cardiomyocytes were treated with $CoCl_2$ with or without 17-AAG at the indicated concentration. **E through G,** 17-AAG inhibits $CoCl_2$-induced p53 accumulation **(E)** and apoptosis in cardiomyocytes, which is abrogated by CHIP knockdown. Neonatal rat cardiomyocytes were transfected with control siRNA or siRNA against CHIP. Twenty-four hours later, medium was changed and the cells were treated with $CoCl_2$ and/or 17-AAG. Apoptosis is assessed by cleaved PARP expression **(E)**, Annexin V staining **(F)**, and caspase-3 activity **(G)**. *$P<0.01$ vs Co; **$P<0.05$ vs Co +17-AAG; n=3.

We also examined whether treatment with 17-AAG exerts similar cardioprotective effects. 17-AAG (10 mg/kg) or vehicle was intraperitoneally injected immediately after permanent coronary artery ligation. This single injection of 17-AAG effectively suppressed the elevation of p53 protein levels and apoptotic cell death in the border zone of the infarct area at 24 hours after the operation (Figure 6A and 6B). As p53 protein level was kept elevated even 4 and 7 days after MI (Figure 2B), 17-AAG was injected every other days and we assessed whether 17-AAG treatment also leads to attenuation of ventricular remodeling, as observed in CHIP-Tg mice. At day 14, mice treated with 17-AAG exhibited smaller HW/BW ratio, better contractility,

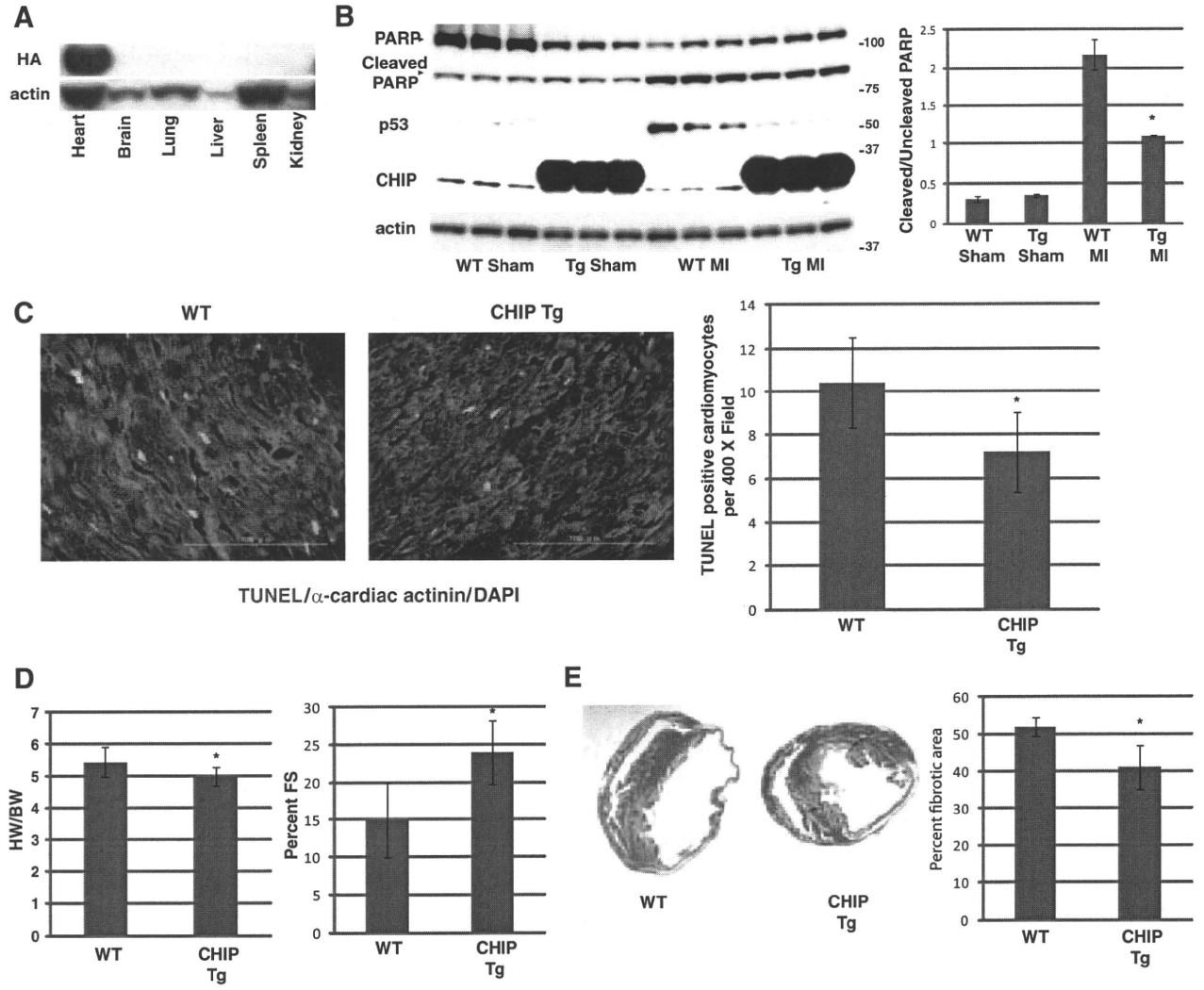

Figure 5. Overexpression of CHIP attenuates ischemic cardiac injury in vivo. A, Cardiac-specific expression of HA-tagged human CHIP in CHIP-Tg mice. **B and C,** p53 accumulation **(B)** and apoptosis 1 day after MI are reduced in CHIP-Tg mice. Apoptosis was assessed by cleaved PARP expression **(B)** and TUNEL staining **(C).** Cleaved PARP level was assessed by densitometric analysis on band intensity of cleaved PARP over uncleaved PARP. $P<0.05$ vs WT; n=3. WT indicates wild-type mice. **D and E,** Postinfarct cardiac remodeling is attenuated in CHIP-Tg mice (n=15). HW/BW ratio **(D, left),** contractile function **(D, right),** and percentage fibrotic area **(E).** *$P<0.01$ vs WT (n=30).

and less ventricular remodeling (Figure 6C and 6D). Interestingly, the effects of 17-AAG were greater than CHIP overexpression (compare Figures 5 and 6), suggesting that 17-AAG possesses cardioprotective activities that do not involve CHIP-mediated p53 degradation. As protein stability of cardioprotective proteins such as Hsp70 and HSF-1 was increased in vitro (Online Figure IV, B and C), we have examined the expression of these proteins in 17-AAG–treated mice. As expected, expression of these two proteins were increased by 17-AAG treatment (Online Figure IV, D), indicating that 17-AAG exerts its antiapoptotic effects by at least two mechanisms, one by inducing CHIP-mediated p53 degradation and the other by increasing cardioprotective heat shock proteins.

Finally, we examined the contribution of CHIP-mediated p53 degradation on the cardioprotective effects of 17-AAG. For that purpose we used CHIP heterozygous mice. There were no differences in cleaved PARP level (Figure 7A; compare WT Sham and Het Sham) or cardiac function between CHIP heterozygous mice and wild-type littermates at the basal level (Table). Following coronary artery ligation, however, apoptotic cell death was observed more prominently in CHIP heterozygous mice as assessed by increased cleaved PARP level (Figure 7A; compare WT MI and Het MI) and increased TUNEL positive cells (Figure 7B). The level of p53 accumulation was comparable following myocardial infarction between wild-type and CHIP heterozygous mice, suggesting the presence of p53 independent mechanisms for enhanced apoptosis caused by CHIP haploinsufficiency. Chronically, CHIP heterozygous mice showed worse cardiac function and worse ventricular remodeling compared with wild-type mice (Figure 7C and 7D). 17-AAG treatment was less effective to reduce p53 protein level, cleaved PARP level (Figure 7A; compare Het MI and Het MI 17-AAG), and TUNEL positive cardiomyocytes in CHIP heterozygous mice, possibly as a result of CHIP haploinsufficiency. 17-AAG treatment had minimal effects on improvements of cardiac function and ventricular remodeling on CHIP heterozygous mice also in the chronic phase (Figure 7C and 7D).

However, we must emphasize that the effects of 17-AAG were not fully attributable to CHIP-mediated p53 degradation

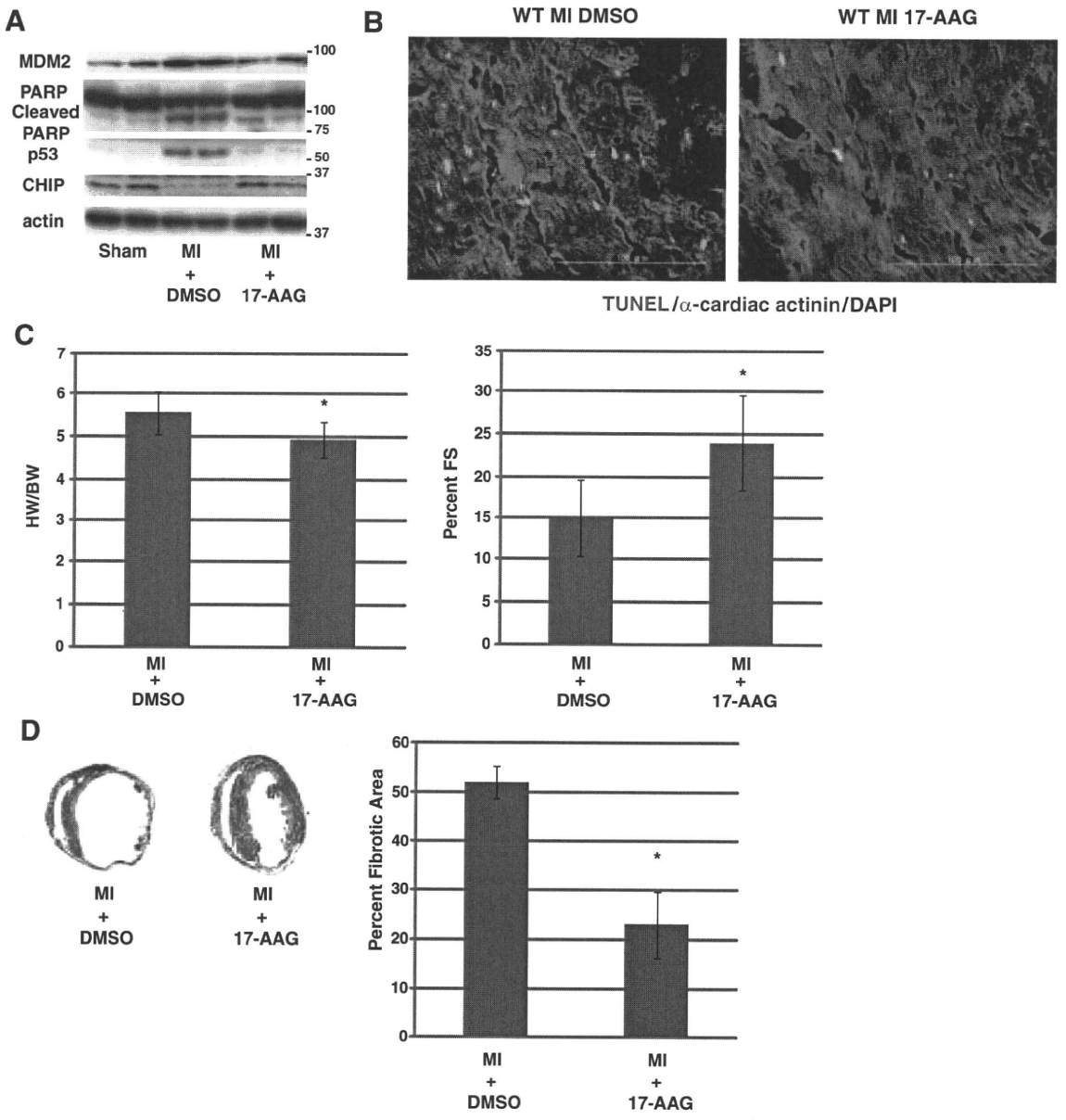

Figure 6. 17-AAG treatment attenuates ischemic cardiac injury in vivo. A, Accumulation of p53 and cleaved PARP in the heart after MI are reduced by 17-AAG treatment. 17-AAG (10 mg/kg) or vehicle was injected immediately after coronary ligation. **B,** Apoptotic cardiomyocytes at 1 day after MI was reduced in 17-AAG–treated mice. Apoptosis was assessed by TUNEL staining. **C and D,** Postinfarct cardiac remodeling is attenuated by 17-AAG treatment (n=20). HW/BW ratio **(C, left)**, contractile function **(C, right)**, and fibrotic area **(D)**. *$P<0.001$; vs MI+DMSO (n=30).

because upregulation of heat shock proteins by 17-AAG was also impaired in CHIP heterozygous mice (Figure 7A; compare WT MI 17-AAG and Het MI 17-AAG). Therefore, it would be fair to conclude that 17-AAG exerts multiple cardioprotective effects after myocardial infarction and at least one of its effects were mediated by promotion of CHIP-mediated p53 degradation.

Discussion

In the present study, we found that accumulation of p53 protein after myocardial ischemia is initiated by HIF-1 dependent downregulation of CHIP level. We have found that CHIP overexpression decreased the amount of p53 and prevented myocardial apoptosis and ameliorated ventricular remodeling after myocardial infarction. We have also found that Hsp90 inhibitor, 17-AAG, exerted similar antiapoptotic and cardioprotective effects after myocardial infarction and showed that these effects of 17-AAG was at least in part mediated by promotion of CHIP-mediated p53 degradation.

Although hypoxic stimuli have been reported to raise p53 protein levels in a variety of cell types, molecular mechanisms of p53 accumulation have been largely unknown. In the present study, we unveiled that downregulation of CHIP protein is critically involved in this process. We found that CHIP expression was downregulated after hypoxic stress through HIF-1–mediated suppression of *CHIP* promoter (Figure 2). We also found that overexpression of CHIP attenuated the p53 accumulation after hypoxic stress (Figures 4A and 5B). These results

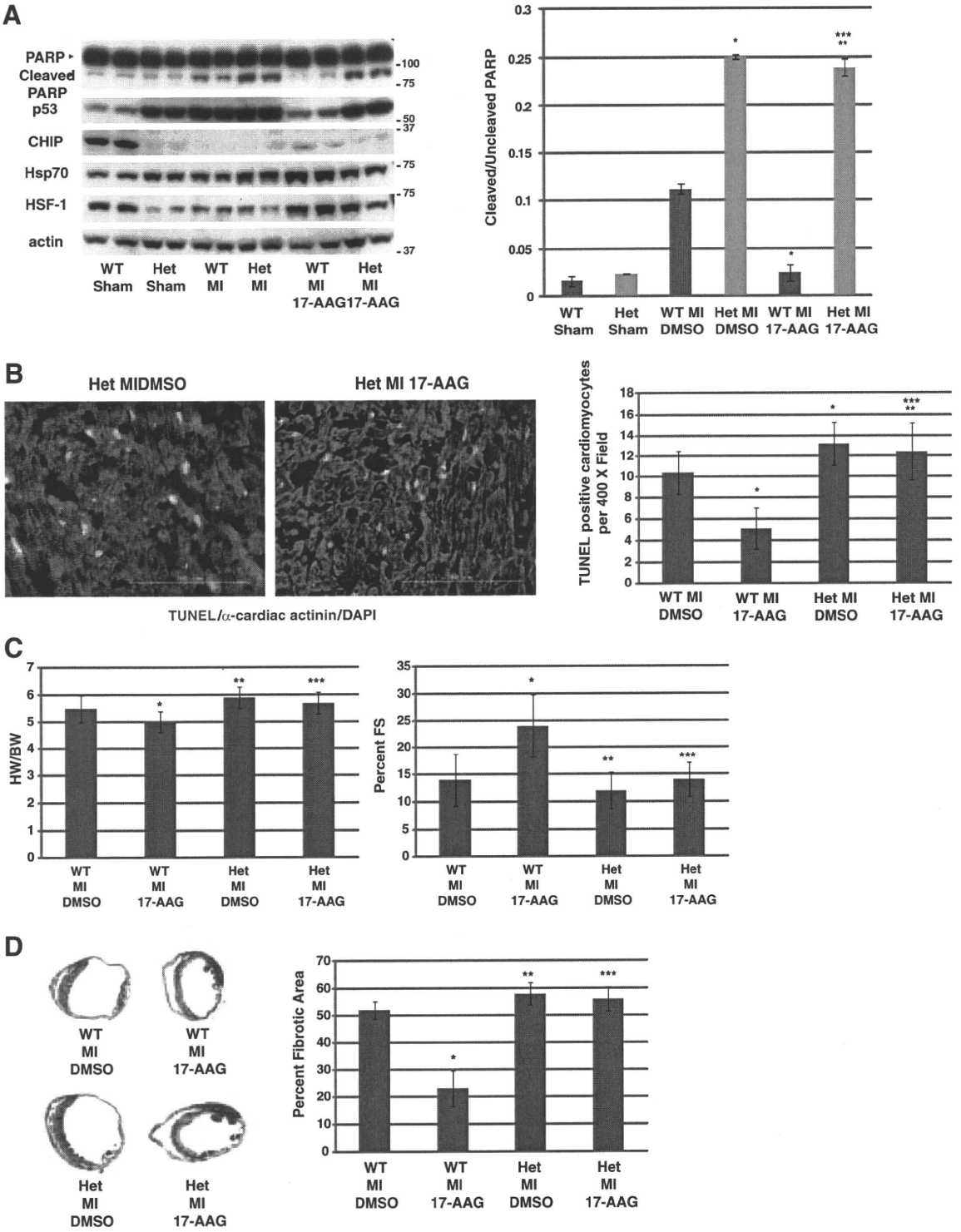

Figure 7. The effect of 17-AAG was dependent on CHIP-mediated p53 degradation and upregulation of heat shock proteins. A, 17-AAG–induced reduction of p53 accumulation and PARP expression was not observed in the heart of CHIP heterozygous mice (Het). Notably, upregulation of heat shock proteins by 17-AAG was ameliorated in CHIP heterozygous mice. **B,** Apoptotic cardiomyocytes on 1 day after MI was reduced in 17-AAG–treated mice, but this antiapoptotic effect of 17-AAG after MI was ameliorated in CHIP heterozygous mice. Apoptosis was assessed by cleaved PARP expression **(A)** and TUNEL staining **(B)**. *$P<0.01$ vs WT+MI+DMSO; **$P<0.01$ vs WT+MI +17-AAG; ***P=NS vs Het+MI+DMSO n=5. WT indicates wild-type mice; Het, CHIP heterozygous mice. **C,** 17-AAG–induced attenuation of postinfarct cardiac remodeling is less in CHIP hetero knockout mice than in wild-type mice. HW/BW ratio **(C, left)**, contractile function **(C, right)**, and fibrotic area **(D)**. *$P<0.001$; **$P<0.05$ vs WT+MI+DMSO; ***P=NS vs Het+MI+DMSO. WT+MI+DMSO: n=30; WT+MI +17-AAG: n=20; Het+MI+DMSO: n=15; Het+MI +17-AAG: n=15. WT indicates wild-type mice.

Table. Basal Characterization of the Mice Used in this Study

	Body Weight (g)	LVEDD (mm)	LVESD (mm)	IVS (mm)	LVPW (mm)	%FS
Wild type	26.3±1.2	3.12±0.12	1.04±0.02	0.72±0.02	0.74±0.02	66.7±1.3
CHIP hetero KO	25.6±0.8	3.10±0.08	1.05±0.03	0.74±0.03	0.78±0.02	66.1±0.8
CHIP Tg	26.9±1.5	3.14±0.16	1.05±0.04	0.75±0.02	0.75±0.05	66.6±1.8

suggest that hypoxic stress downregulates CHIP, leading to decreased CHIP-mediated proteolysis of p53 protein and accumulation of p53 protein. This mechanism seems to be a 'fine-tuning' of HIF-1 activity because p53 protein has been reported to bind to and inhibit HIF-1 activity.[16] After hypoxia, first HIF-1 accumulates and induces angiogenic genes, to promote angiogenesis. Thereafter, as a negative feedback loop, HIF-1 induces downregulation of *CHIP* expression and p53 accumulates, then accumulated p53 inhibits HIF-1 activity.[35] In general, this feedback system might have an antitumor effect, because in many tumor cells HIF-1 induces feeding vessels in hypoxic tumors and promotes tumor growth. HIF-1-induced, CHIP-mediated p53 accumulation acts to suppress tumor growth by (1) suppressing HIF-1 activity and blocking neovascularization and (2) inducing p53-mediated apoptosis of tumor cells. However, in the heart, this negative feedback system worsens hypoxic situation by blocking neovascularization[16] and by inducing apoptosis (this study).

The important role of apoptosis in the progression of ventricular remodeling and the possibility of antiapoptotic approach against heart failure has already been elegantly shown by Wencker et al.[3] Antiapoptotic approach after myocardial infarction has been reported to be cardioprotective not only in ischemia-reperfusion model but also in permanent coronary ligation model.[21,36,37] Therefore, inhibition of apoptotic death does not only reduce initial infarct size but also prevents ventricular remodeling through inhibiting apoptosis in the border zone of the infarct.

Accumulation of p53 has been reported to initiate many proapoptotic triggers.[38] In the heart, p53 accumulates (Figure 3C) and p53-dependent apoptosis occurs[39] after permanent coronary occlusion. We have also observed that *p53* gene deletion lead to less ventricular remodeling after myocardial infarction.[16] In the present study, we have shown that CHIP overexpression or 17-AAG treatment could prevent cardiomyocyte apoptosis and ameliorate ventricular remodeling after myocardial infarction. We have also shown some evidences that inhibition of p53 accumulation is at least one of the mechanisms for the effect of CHIP overexpression and 17-AAG. However, it should be noted that Hsp90 chaperones various proteins including prosurvival factors such as Akt/protein kinase B[40] in tumor cells and that Hsp90 inhibitors induced degradation of aberrantly overexpressed prosurvival factors in those tumor cells. Although the nature of the effects of 17-AAG seems to induce degradation of aberrantly expressed proteins, it is also possible and taken into account that 17-AAG could also induce degradation of prosurvival factors and play detrimental effects in cardiomyocytes.

In conclusion, our observations indicate that investigation of novel anti-p53 approach would open a way toward new treatment of myocardial infarction.

Acknowledgments

We thank Y. Ohtsuki, I. Sakamoto, M. Ikeda, and A. Furuyama for excellent technical support.

Sources of Funding

This work was supported by a Grant-in-Aid for Scientific Research on Priority Areas and for Exploratory Research (Ministry of Education, Culture, Sports, Science and Technology), Health and Labour Sciences Research grants (to I.K.), and research fellowships from the Japan Society for the Promotion of Science for Young Scientists (to A.T.N.). A.T.N. is a research fellow of the Japan Society for the Promotion of Science.

Disclosures

None.

References

1. Rosamond W, Flegal K, Friday G, Furie K, Go A, Greenlund K, Haase N, Ho M, Howard V, Kissela B, Kittner S, Lloyd-Jones D, McDermott M, Meigs J, Moy C, Nichol G, O'Donnell CJ, Roger V, Rumsfeld J, Sorlie P, Steinberger J, Thom T, Wasserthiel-Smoller S, Hong Y. Heart disease and stroke statistics–2007 update: a report from the American Heart Association Statistics Committee and Stroke Statistics Subcommittee. *Circulation.* 2007;115:e69–e171.
2. Kajstura J, Cheng W, Reiss K, Clark WA, Sonnenblick EH, Krajewski S, Reed JC, Olivetti G, Anversa P. Apoptotic and necrotic myocyte cell deaths are independent contributing variables of infarct size in rats. *Lab Invest.* 1996;74:86–107.
3. Wencker D, Chandra M, Nguyen K, Miao W, Garantziotis S, Factor SM, Shirani J, Armstrong RC, Kitsis RN. A mechanistic role for cardiac myocyte apoptosis in heart failure. *J Clin Invest.* 2003;111:1497–1504.
4. Haunstetter A, Izumo S. Toward antiapoptosis as a new treatment modality. *Circ Res.* 2000;86:371–376.
5. Chatterjee S, Stewart AS, Bish LT, Jayasankar V, Kim EM, Pirolli T, Burdick J, Woo YJ, Gardner TJ, Sweeney HL. Viral gene transfer of the antiapoptotic factor Bcl-2 protects against chronic postischemic heart failure. *Circulation.* 2002;106:I212–I217.
6. Hochhauser E, Kivity S, Offen D, Maulik N, Otani H, Barhum Y, Pannet H, Shneyvays V, Shainberg A, Goldshtaub V, Tobar A, Vidne BA. Bax ablation protects against myocardial ischemia-reperfusion injury in transgenic mice. *Am J Physiol Heart Circ Physiol.* 2003;284:H2351–H2359.
7. Imahashi K, Schneider MD, Steenbergen C, Murphy E. Transgenic expression of Bcl-2 modulates energy metabolism, prevents cytosolic acidification during ischemia, and reduces ischemia/reperfusion injury. *Circ Res.* 2004;95:734–741.
8. Hochhauser E, Cheporko Y, Yasovich N, Pinchas L, Offen D, Barhum Y, Pannet H, Tobar A, Vidne BA, Birk E. Bax deficiency reduces infarct size and improves long-term function after myocardial infarction. *Cell Biochem Biophys.* 2007;47:11–20.
9. Vogelstein B, Lane D, Levine AJ. Surfing the p53 network. *Nature.* 2000;408:307–310.
10. Haupt Y, Maya R, Kazaz A, Oren M. Mdm2 promotes the rapid degradation of p53. *Nature.* 1997;387:296–299.
11. Kubbutat MH, Jones SN, Vousden KH. Regulation of p53 stability by Mdm2. *Nature.* 1997;387:299–303.
12. Dornan D, Wertz I, Shimizu H, Arnott D, Frantz GD, Dowd P, O'Rourke K, Koeppen H, Dixit VM. The ubiquitin ligase COP1 is a critical negative regulator of p53. *Nature.* 2004;429:86–92.
13. Leng RP, Lin Y, Ma W, Wu H, Lemmers B, Chung S, Parant JM, Lozano G, Hakem R, Benchimol S. Pirh2, a p53-induced ubiquitin-protein ligase, promotes p53 degradation. *Cell.* 2003;112:779–791.
14. Long X, Boluyt MO, Hipolito ML, Lundberg MS, Zheng JS, O'Neill L, Cirielli C, Lakatta EG, Crow MT. p53 and the hypoxia-induced apoptosis

of cultured neonatal rat cardiac myocytes. *J Clin Invest.* 1997;99: 2635–2643.
15. Liu P, Xu B, Cavalieri TA, Hock CE. Pifithrin-alpha attenuates p53-mediated apoptosis and improves cardiac function in response to myocardial ischemia/reperfusion in aged rats. *Shock.* 2006;26:608–614.
16. Sano M, Minamino T, Toko H, Miyauchi H, Orimo M, Qin Y, Akazawa H, Tateno K, Kayama Y, Harada M, Shimizu I, Asahara T, Hamada H, Tomita S, Molkentin JD, Zou Y, Komuro I. p53-induced inhibition of Hif-1 causes cardiac dysfunction during pressure overload. *Nature.* 2007; 446:444–448.
17. Song K, Backs J, McAnally J, Qi X, Gerard RD, Richardson JA, Hill JA, Bassel-Duby R, Olson EN. The transcriptional coactivator CAMTA2 stimulates cardiac growth by opposing class II histone deacetylases. *Cell.* 2006;125:453–466.
18. Zou Y, Komuro I, Yamazaki T, Kudoh S, Uozumi H, Kadowaki T, Yazaki Y. Both Gs and Gi proteins are critically involved in isoproterenol-induced cardiomyocyte hypertrophy. *J Biol Chem.* 1999;274:9760–9770.
19. Sohal DS, Nghiem M, Crackower MA, Witt SA, Kimball TR, Tymitz KM, Penninger JM, Molkentin JD. Temporally regulated and tissue-specific gene manipulations in the adult and embryonic heart using a tamoxifen-inducible Cre protein. *Circ Res.* 2001;89:20–25.
20. Sahara N, Murayama M, Mizoroki T, Urushitani M, Imai Y, Takahashi R, Murata S, Tanaka K, Takashima A. In vivo evidence of CHIP up-regulation attenuating tau aggregation. *J Neurochem.* 2005;94:1254–1263.
21. Harada M, Qin Y, Takano H, Minamino T, Zou Y, Toko H, Ohtsuka M, Matsuura K, Sano M, Nishi J, Iwanaga K, Akazawa H, Kunieda T, Zhu W, Hasegawa H, Kunisada K, Nagai T, Nakaya H, Yamauchi-Takihara K, Komuro I. G-CSF prevents cardiac remodeling after myocardial infarction by activating the Jak-Stat pathway in cardiomyocytes. *Nat Med.* 2005;11:305–311.
22. McDonough H, Patterson C. CHIP: a link between the chaperone and proteasome systems. *Cell Stress Chaperones.* 2003;8:303–308.
23. Esser C, Scheffner M, Hohfeld J. The chaperone-associated ubiquitin ligase CHIP is able to target p53 for proteasomal degradation. *J Biol Chem.* 2005;280:27443–27448.
24. Tripathi V, Ali A, Bhat R, Pati U. CHIP chaperones wild type p53 tumor suppressor protein. *J Biol Chem.* 2007;282:28441–28454.
25. Graeber TG, Peterson JF, Tsai M, Monica K, Fornace AJ Jr, Giaccia AJ. Hypoxia induces accumulation of p53 protein, but activation of a G1-phase checkpoint by low-oxygen conditions is independent of p53 status. *Mol Cell Biol.* 1994;14:6264–6277.
26. An WG, Kanekal M, Simon MC, Maltepe E, Blagosklonny MV, Neckers LM. Stabilization of wild-type p53 by hypoxia-inducible factor 1alpha. *Nature.* 1998;392:405–408.
27. Chen KF, Lai YY, Sun HS, Tsai SJ. Transcriptional repression of human cad gene by hypoxia inducible factor-1alpha. *Nucleic Acids Res.* 2005; 33:5190–5198.
28. Eltzschig HK, Abdulla P, Hoffman E, Hamilton KE, Daniels D, Schonfeld C, Loffler M, Reyes G, Duszenko M, Karhausen J, Robinson A, Westerman KA, Coe IR, Colgan SP. HIF-1-dependent repression of equilibrative nucleoside transporter (ENT) in hypoxia. *J Exp Med.* 2005;202:1493–1505.
29. Ibla JC, Khoury J, Kong T, Robinson A, Colgan SP. Transcriptional repression of Na-K-2Cl cotransporter NKCC1 by hypoxia-inducible factor-1. *Am J Physiol Cell Physiol.* 2006;291:C282–C289.
30. Bindra RS, Glazer PM. Co-repression of mismatch repair gene expression by hypoxia in cancer cells: role of the Myc/Max network. *Cancer Lett.* 2007;252:93–103.
31. Waza M, Adachi H, Katsuno M, Minamiyama M, Sang C, Tanaka F, Inukai A, Doyu M, Sobue G. 17-AAG, an Hsp90 inhibitor, ameliorates polyglutamine-mediated motor neuron degeneration. *Nat Med.* 2005;11: 1088–1095.
32. Dickey CA, Kamal A, Lundgren K, Klosak N, Bailey RM, Dunmore J, Ash P, Shoraka S, Zlatkovic J, Eckman CB, Patterson C, Dickson DW, Nahman NS Jr, Hutton M, Burrows F, Petrucelli L. The high-affinity HSP90-CHIP complex recognizes and selectively degrades phosphorylated tau client proteins. *J Clin Invest.* 2007;117:648–658.
33. Suzuki K, Sawa Y, Kaneda Y, Ichikawa H, Shirakura R, Matsuda H. In vivo gene transfection with heat shock protein 70 enhances myocardial tolerance to ischemia-reperfusion injury in rat. *J Clin Invest.* 1997;99:1645–1650.
34. Sakamoto M, Minamino T, Toko H, Kayama Y, Zou Y, Sano M, Takaki E, Aoyagi T, Tojo K, Tajima N, Nakai A, Aburatani H, Komuro I. Upregulation of heat shock transcription factor 1 plays a critical role in adaptive cardiac hypertrophy. *Circ Res.* 2006;99:1411–1418.
35. Blagosklonny MV, An WG, Romanova LY, Trepel J, Fojo T, Neckers L. p53 inhibits hypoxia-inducible factor-stimulated transcription. *J Biol Chem.* 1998;273:11995–11998.
36. Chandrashekhar Y, Sen S, Anway R, Shuros A, Anand I. Long-term caspase inhibition ameliorates apoptosis, reduces myocardial troponin-I cleavage, protects left ventricular function, and attenuates remodeling in rats with myocardial infarction. *J Am Coll Cardiol.* 2004;43:295–301.
37. Balsam LB, Kofidis T, Robbins RC. Caspase-3 inhibition preserves myocardial geometry and long-term function after infarction. *J Surg Res.* 2005;124:194–200.
38. Crow MT, Mani K, Nam YJ, Kitsis RN. The mitochondrial death pathway and cardiac myocyte apoptosis. *Circ Res.* 2004;95:957–970.
39. Matsusaka H, Ide T, Matsushima S, Ikeuchi M, Kubota T, Sunagawa K, Kinugawa S, Tsutsui H. Targeted deletion of p53 prevents cardiac rupture after myocardial infarction in mice. *Cardiovasc Res.* 2006;70: 457–465.
40. Solit DB, Basso AD, Olshen AB, Scher HI, Rosen N. Inhibition of heat shock protein 90 function downregulates Akt kinase and sensitizes tumors to Taxol. *Cancer Res.* 2003;63:2139–2144.

Novelty and Significance

What Is Known?

- Inhibition of myocardial apoptosis after myocardial infarction is cardioprotective.
- p53 expression is increased after myocardial infarction and induces cardiomyocyte apoptosis.

What New Information Does This Article Contribute?

- We identified CHIP as the endogenous p53 antagonist expressed in the heart.
- We found that CHIP downregulation is critically involved in the molecular mechanisms for p53 elevation after myocardial infarction.
- We showed several possibilities of the anti-p53 treatment after myocardial infarction.

Accumulation of tumor suppressor protein p53 in the myocardium causes the transition from adaptive cardiac hypertrophy to heart failure. However, the mechanisms of p53 accumulation in the heart and its therapeutic implications have been elusive. Here we show that downregulation of the chaperone-associated E3 ubiquitin ligase CHIP (carboxyl terminus of Hsp70-interacting protein) mediates hypoxia-induced p53 accumulation in the heart and that promotion of CHIP-induced p53 degradation protects the heart from ischemic injury. Under physiological conditions, CHIP limited the p53 protein amount at low levels by inducing proteasomal degradation of p53. Under hypoxic conditions, hypoxia inducible factor-1 (HIF-1) downregulated CHIP, resulting in the accumulation of p53. Overexpression of CHIP or administration of an Hsp90 inhibitor promoted CHIP-mediated p53 degradation and attenuated ischemic cardiac injury. These results indicate that CHIP is a crucial negative regulator of p53 in the heart and suggest that promotion of CHIP-mediated p53 degradation could be a novel therapeutic strategy for heart diseases.

Ca^{2+}/Calmodulin-Dependent Kinase IIδ Causes Heart Failure by Accumulation of p53 in Dilated Cardiomyopathy

Haruhiro Toko, MD, PhD; Hidehisa Takahashi, MD, PhD; Yosuke Kayama, MD; Toru Oka, MD, PhD; Tohru Minamino, MD, PhD; Sho Okada, MD, PhD; Sachio Morimoto, PhD; Dong-Yun Zhan, PhD; Fumio Terasaki, MD, PhD; Mark E. Anderson, MD, PhD; Masashi Inoue, MD, PhD; Atsushi Yao, MD, PhD; Ryozo Nagai, MD, PhD; Yasushi Kitaura, MD, PhD; Toshiyuki Sasaguri, MD, PhD; Issei Komuro, MD, PhD

Background—Dilated cardiomyopathy (DCM), characterized by dilatation and dysfunction of the left ventricle, is an important cause of heart failure. Many mutations in various genes, including cytoskeletal protein genes and contractile protein genes, have been identified in DCM patients, but the mechanisms of how such mutations lead to DCM remain unknown.

Methods and Results—We established the mouse model of DCM by expressing a mutated cardiac α-actin gene, which has been reported in patients with DCM, in the heart (mActin-Tg). mActin-Tg mice showed gradual dilatation and dysfunction of the left ventricle, resulting in death by heart failure. The number of apoptotic cardiomyocytes and protein levels of p53 were increased in the hearts of mActin-Tg mice. Overexpression of Bcl-2 or downregulation of p53 decreased the number of apoptotic cardiomyocytes and improved cardiac function. This mouse model showed a decrease in myofilament calcium sensitivity and activation of calcium/calmodulin-dependent kinase IIδ (CaMKIIδ). The inhibition of CaMKIIδ prevented the increase in p53 and apoptotic cardiomyocytes and ameliorated cardiac function.

Conclusion—CaMKIIδ plays a critical role in the development of heart failure in part by accumulation of p53 and induction of cardiomyocyte apoptosis in the DCM mouse model. **(*Circulation*. 2010;122:891-899.)**

Key Words: apoptosis ■ CaMKII ■ cardiomyopathy ■ heart failure ■ genes, p53

Heart failure is an important cause of morbidity and mortality in many industrial countries, and dilated cardiomyopathy (DCM) is one of its major causes.[1] Although treatments for heart failure have been progressed well in both pharmacological and nonpharmacological aspects, mortality of DCM patients remains high, and the only treatment for DCM patients with severe symptoms is heart transplantation. Because the number of hearts for transplantation is limited, the development of novel therapies for DCM has been awaited.

Clinical Perspective on p 899

DCM, characterized by dilatation and impaired contraction of the left ventricle, is a multifactorial disease that includes both hereditary and acquired forms. The acquired forms of DCM are caused by various factors.[2] Twenty percent to 35% of patients have hereditary forms,[1] and advances in molecular genetic studies during the last decade have revealed many mutations of various genes in DCM patients.[3–5]

Several hypotheses have been reported on the mechanisms of how gene mutations lead to DCM phenotypes. Mutations in genes encoding cytoskeletal proteins such as desmin and muscle LIM protein might disturb the interaction between the sarcomere and Z disk, resulting in impaired force transmission from the sarcomere to the surrounding syncytium.[4,6] On the other hand, mutations in genes encoding contractile proteins such as α-tropomyosin and cardiac troponin T have been reported to induce the decrease in myofilament calcium (Ca^{2+}) sensitivity.[7] An increase in apoptotic cardiomyocytes and/or destruction of membrane structure by calpain activa-

Received January 6, 2010; accepted July 2, 2010.

From the Department of Cardiovascular Science and Medicine, Chiba University Graduate School of Medicine, Chiba, Japan (H. Toko, H. Takahashi, Y.K., T.O., T.M., S.O., I.K.); Department of Cardiovascular Medicine, Osaka University Graduate School of Medicine, Suita, Japan (T.O., I.K.); Department of Clinical Pharmacology, Kyusyu University Graduate School of Medicine, Fukuoka, Japan (S.M., D.Z., T.S.); Department of Internal Medicine III, Osaka Medical College, Takatsuki, Japan (F.T., Y.K.); Department of Internal Medicine, and Molecular Physiology and Biophysics, Carver College of Medicine, University of Iowa, Iowa City (M.E.A.); and Department of Cardiovascular Medicine, University of Tokyo Graduate School of Medicine, Tokyo, Japan (M.I., A.Y., R.N.).

The online-only Data Supplement is available with this article at http://circ.ahajournals.org/cgi/content/full/CIRCULATIONAHA.109.935296/DC1.

Correspondence to Issei Komuro, MD, PhD, Department of Cardiovascular Medicine, Osaka University Graduate School of Medicine, 2-2 Yamadaoka, Suita 565-0871, Japan. E-mail komuro-tky@umin.ac.jp

Circulation **is available at http://circ.ahajournals.org** **DOI: 10.1161/CIRCULATIONAHA.109.935296**

tion have been reported to play a critical role in mutant gene–induced cardiac dysfunction.[8–10] However, the precise mechanisms remain largely unknown as a result, at least in part, of a lack of good animal models of DCM.

Several animal models of DCM have been reported.[11–13] The *mdx* mouse is a model of Duchenne muscular dystrophy, which has mutations in the dystrophin gene.[11] Unlike humans, *mdx* mice rarely show cardiac abnormality, which has limited the utility of *mdx* mice as a model to examine the pathogenesis of DCM. Although Golden Retriever–based muscular dystrophy dogs show DCM phenotypes,[12] the muscular dystrophy dogs are very difficult to maintain and handle. Although BIO 14.6 hamsters lacking δ-sarcoglycan are a good model of DCM,[13] it is difficult to apply genetic approaches to the hamster. To elucidate the molecular mechanisms of how gene mutations cause DCM, appropriate animal models, particularly mouse models, are necessary. We established here a mouse model of DCM by expressing a mutated cardiac α-actin gene (mActin-Tg), which has been reported in patients with DCM, in the heart.[5] mActin-Tg mice showed gradual dilatation and dysfunction of the left ventricle, resulting in death by heart failure. These phenotypes of mActin-Tg mice were quite similar to those of human DCM. In this study, we examined the underlying mechanisms of how this gene mutation leads to DCM using the new mouse model of DCM.

Methods

Detailed experimental methods are described in the online-only Data Supplement.

Mice

We generated transgenic mice (mActin-Tg) that expressed a mutated cardiac α-actin (R312H) with an HA tag in the heart. This mutation has been reported in patients with DCM.[5] Generation of transgenic mice with cardiac-restricted overexpression of human Bcl-2, AC3-I, or nuclear factor of activated T cell (NFAT)–luciferase has been described previously.[14–16] Heterozygous p53-deficient mice were purchased from The Jackson Laboratory (Bar Harbor, Me).[17] Wild-type littermates served as controls for all studies. KN-93 (10 μmol · kg^{-1} · $/d^{-1}$) was used to inhibit activation of Ca^{2+}/calmodulin-dependent kinase II (CaMKII). Echocardiography was performed on conscious mice.

Histology

For detection of apoptotic cardiomyocytes, we performed terminal deoxynucleotidyl transferase–mediated dUTP nick-end labeling (TUNEL) staining, along with immunostaining for dystrophin.

Western Blot Analysis

Whole-cell lysates were resolved by SDS-PAGE. Western blot analyses were performed with some antibodies. The intensities of Western blot bands were measured with NIH ImageJ software (National Institutes of Health, Bethesda, Md).

Luciferase Assay

Left ventricles were homogenized in luciferase assay buffer as described previously.[15]

Force Measurements

A small fiber was dissected from the skinned left ventricular papillary muscle, and isometric force was measured as described previously.[7]

RNA Extraction and Quantitative Real-Time Polymerase Chain Reaction Analysis

Quantitative real-time polymerase chain reaction was performed with the LightCycler with the Taqman Universal Probe Library and Light Cycler Master. Relative levels of gene expressions were normalized to the mouse GAPDH expression with the ΔΔCt method.[18]

Statistical Analysis

Data are shown as mean±SEM. Multiple-group comparison was performed by 1-way ANOVA followed by the Bonferroni procedure for comparison of means. The F test was used to assess equal variances before comparison between 2 groups. Then, comparisons between 2 groups were performed with the Student t test (when $P>0.05$ in the F test) and the Welch t test (when $P<0.05$ in the F test). Survival rates were analyzed with the log-rank test. Values of $P<0.05$ were considered statistically significant.

Results

DCM Model Mouse

Because there are few useful DCM mouse models, we first generated transgenic mice that expressed a cardiac α-actin R312H mutant with an HA tag under the control of α-myosin heavy chain promoter (mActin-Tg). We obtained 3 independent founders of the transgenic mice (lines 301, 307, and 311). The protein levels of the cardiac α-actin R312H mutant were 1.6-fold in line 301, 3.3-fold in line 307, and 2.2-fold in line 311 compared with those of endogenous cardiac α-actin (Figure IA in the online-only Data Supplement). To confirm the expression of the transgene in cardiomyocytes, we performed immunohistological analyses with antibodies against HA and actinin. The mutated cardiac α-actin protein was colocalized with actinin, suggesting that the cardiac α-actin R312H mutant is incorporated into myofilaments (Figure IB in the online-only Data Supplement). Cardiac systolic function was decreased in mActin-Tg mice at 10 months of age, and the reduction was well correlated with protein levels of the cardiac α-actin R312H mutant (Figure IC in the online-only Data Supplement). To further investigate whether cardiac expression of the cardiac α-actin R312H mutant led to heart failure, we examined another transgenic mouse that expressed cardiac α-actin A331P mutant with an HA tag in the heart. This mutant has been reported to cause hypertrophic cardiomyopathy in human.[19] We obtained 2 independent founders of the transgenic mice that expressed almost the same levels of the cardiac α-actin A331P mutant protein. Although the protein levels of the mutant in the A331P mutant transgenic mice were almost same as those of the R312H mutant in line 307, which had the highest expression (Figure II in the online-only Data Supplement), echocardiography revealed that there were no significant differences in cardiac systolic function, wall thickness, and left ventricular dimension between cardiac α-actin A331P mutant transgenic mice and their wild-type littermates (Table I in the online-only Data Supplement). Although it is not known at present why the expression of cardiac α-actin A331P mutant did not induce hypertrophic cardiomyopathy, these results suggest that cardiac dysfunction of mActin-Tg mice is due to cardiac expression of the cardiac α-actin R312H mutant in the heart, not to high-level expression of the cardiac α-actin protein with the tag (lines 307 and 311).

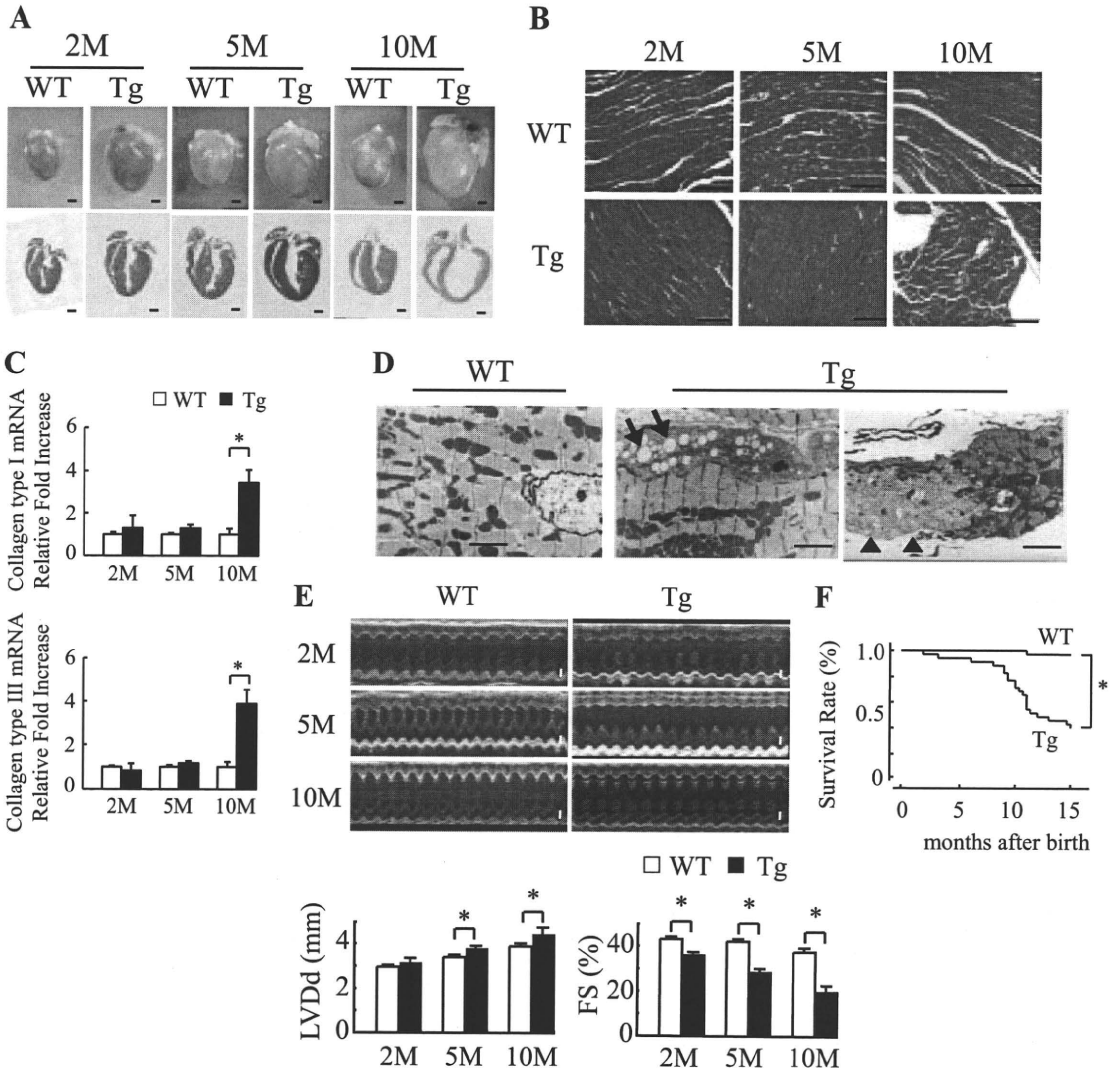

Figure 1. Mutated cardiac α-actin R312H transgenic mice. A, Gross morphology (top) and sections (bottom) of wild-type littermates (WT) or mActin-Tg (Tg) hearts at 2, 5, and 10 months (M) of age. Scale bar=1 mm. B, Masson trichrome staining. Scale bar=100 μm. C, Relative levels of collagen types I and III in hearts were normalized to GAPDH expression. *$P<0.05$ vs WT mice. n=4 in each group. D, Electron microscopic analyses. Cytoplasmic vacuolization (arrow) and lysis of myofibrils (arrowhead) were detected in the hearts of Tg mice. Scale bar=10 μm. E, Echocardiographic analysis. Scale bar=1 mm. LVDd indicates left ventricular end-diastolic dimension; FS, fractional shortening. *$P<0.05$. F, Kaplan-Meier survival curve. *$P<0.05$ vs WT mice. WT, n=32; Tg, n=37.

We used line 307, which expressed the cardiac α-actin R312H mutant at the highest levels, for further studies. The hearts in mActin-Tg mice were larger than those of wild-type littermates (Figure 1A), and heart weight and the ratio of heart weight to body weight were much increased in mActin-Tg mice (Table II in the online-only Data Supplement). Marked cardiac fibrosis was observed in mActin-Tg mice at 10 months of age, with increased expression of collagen types I and III (Figure 1B and 1C). Electron microscopic analyses showed that there were degenerated cardiomyocytes with an increase in vacuolar formation and lysis of myofibrils in mActin-Tg mice (Figure 1D). Echocardiography revealed that left ventricular dimension was gradually increased and that fractional shortening was reduced in mActin-Tg mice compared with wild-type littermates (Table II in the online-only Data Supplement and Figure 1E). The expression levels of ANP and SERCA2a were gradually increased and decreased in mActin-Tg mice, respectively (Figure III in the online-only Data Supplement). There was no significant difference in blood pressure, but heart rate was increased in mActin-Tg mice (Table II in the online-only Data Supplement), suggesting that the sympathetic nervous system is activated. Surface ECG monitoring showed low amplitude of the R wave in mActin-Tg mice (Table II in the online-only Data Supplement), which is often observed in human DCM patients. Many mActin-Tg mice died by 35 weeks of age (Figure 1F). Although telemetric ECG recording did not show life-threatening arrhythmia in mActin-Tg mice (data not shown), spontaneous Ca^{2+} sparks and Ca^{2+} waves were significantly increased in the cardiomyocytes of mActin-Tg mice (Table III in the online-only Data Supplement), suggesting that not only cardiac pump failure but also arrhythmia could be the cause of death. These phenotypes of mActin-Tg mice were quite similar to those of human DCM.

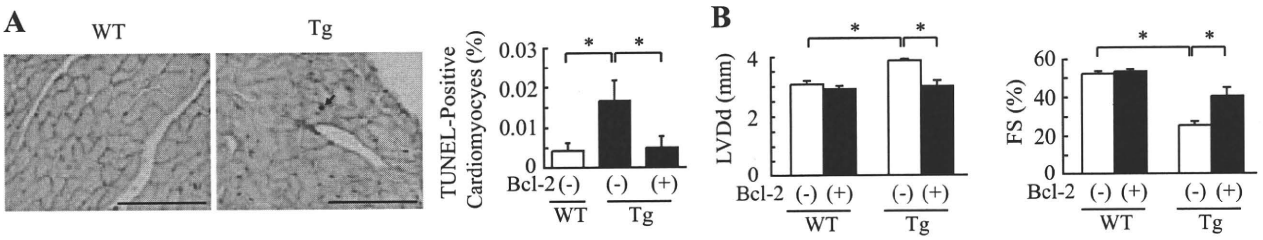

Figure 2. Increase in Bcl-2 preserves cardiac function in mActin-Tg mice. A, Double immunostaining for TUNEL (black) and dystrophin (red) of the heart (left). The graph indicates quantitative analyses of TUNEL-positive cardiomyocytes. Scale bar=100 μm. n=4 in each group. *$P<0.05$. B, Echocardiographic analyses at 5 months of age. *$P<0.05$. WT/Bcl-2(−), n=5; WT/Bcl-2(+), n=10; Tg/Bcl-2(−), n=10; Tg/Bcl-2(+), n=5. WT indicates wild-type littermates; Tg, mActin-Tg mice; LVDd, left ventricular end-diastolic dimension; and FS, fractional shortening.

Apoptotic Cardiomyocytes Are Increased in mActin-Tg Hearts

It has been reported that apoptosis of cardiomyocytes is observed in hearts of human DCM[10] and that cardiomyocyte death might cause cardiac dysfunction.[20] We thus examined apoptosis of cardiomyocytes by TUNEL labeling in left ventricular sections of wild-type littermates and mActin-Tg mice at 5 months of age. The number of TUNEL/dystrophin double-positive cardiomyocytes was significantly larger in mActin-Tg mice compared with wild-type littermates (Figure 2A). To examine whether the increase in apoptotic cardiomyocytes causes cardiac dysfunction in mActin-Tg mice, we generated double-transgenic mice by crossing mActin-Tg mice and the transgenic mice, which overexpress the antiapoptotic protein Bcl-2 in cardiomyocytes [mActin(+)/Bcl-2(+)-DTg].[14] The number of apoptotic cardiomyocytes in mActin(+)/Bcl-2(+)-DTg mice was significantly less compared with mActin-Tg mice (Figure 2A). Echocardiography revealed that the left ventricular dimension was smaller and fractional shortening was better in mActin(+)/Bcl-2(+)-DTg mice than in mActin-Tg mice at 5 months of age (Figure 2B), suggesting that the increase in apoptotic cardiomyocytes causes cardiac dysfunction in the DCM mouse model.

p53 Is Involved in Cardiomyocyte Apoptosis in mActin-Tg Mice

To clarify the mechanisms of how the cardiac α-actin R312H mutant induces apoptosis of cardiomyocytes, we examined expression levels of apoptosis-related proteins by Western blot analyses. The protein levels of p53 and Bax were higher in mActin-Tg mice compared with wild-type littermates (Figure 3A). Several key proapoptotic genes have been reported to be positively regulated by p53,[21] and increased expression of p53 induces left ventricular dilatation and dysfunction in several types of mice.[22,23] To determine the role of p53 in gene mutation–induced DCM, we crossed mActin-Tg mice and heterozygous p53-deficient mice [p53(+/−)]. Because many of homozygous p53-deficient mice [p53(−/−)] died of tumors before 5 months of age,[17] we used heterozygous p53-deficient mice [p53(+/−)] for this study. Echocardiography revealed that left ventricular dimension was smaller and fractional shortening was better in mActin-Tg/p53(+/−) mice than in mActin-Tg/p53(+/+) mice at 5 months of age (Figure 3B). Loss of a single p53 allele attenuated the increase of Bax (Figure 3C) and reduced the number of apoptotic cardiomyocytes in mActin-Tg mice (Figure 3D). These results suggest that p53-induced cardiomyocyte apoptosis induces dilatation and dysfunction of the left ventricle in the DCM mouse model.

Myofilament Calcium Sensitivity Is Decreased and Calcium-Dependent Enzymes Are Activated in mActin-Tg Mice

Many gene mutations associated with DCM have been reported to induce the decrease of myofilament Ca^{2+} sensi-

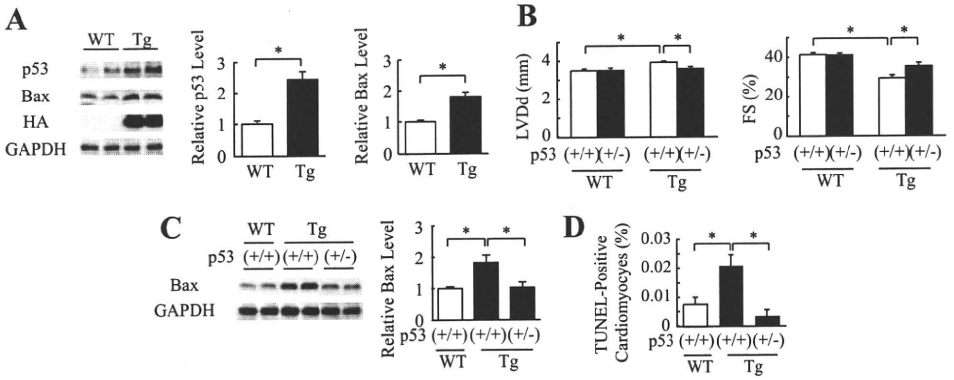

Figure 3. Inhibition of p53 preserves cardiac function in mActin-Tg mice. A, Western blot analyses in the hearts of wild-type littermates (WT) or mActin-Tg (Tg) mice at 5 months of age. The graph indicates relative protein levels of p53 (n=8 in each group) or Bax (n=10 in each group). *$P<0.05$. B, Echocardiographic analyses at 5 months of age. WT/p53(+/+), n=12; WT/p53(+/−), n=10; Tg/p53(+/+), n=19; Tg/p53(+/−), n=14. *$P<0.05$. C, Western blot analyses in the hearts. The graph indicates relative protein levels of Bax. n=6 in each group. *$P<0.05$. D, Quantitative analyses of TUNEL-positive cardiomyocytes. n=5 in each group. *$P<0.05$.

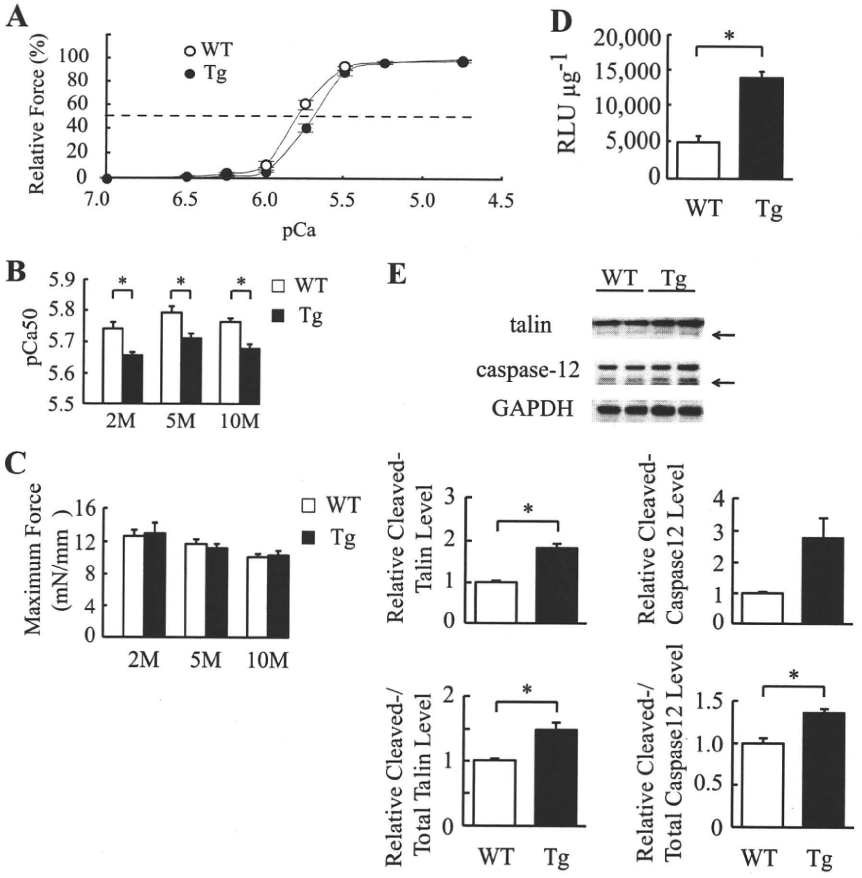

Figure 4. Myofilament Ca^{2+} sensitivity is decreased and Ca^{2+}-dependent enzymes are activated in mActin-Tg mice (Tg). A, Force-pCa relationship in skinned cardiac muscle fiber at 5 months of age. The broken line indicates pCa50. Wild-type (WT; n=11) and Tg (n=10) fibers were prepared from 3 isolated hearts. B, Ca^{2+} sensitivity (pCa50) of force-pCa relationships in skinned cardiac muscle fibers at 2, 5, and 10 months (M) of age. *$P<0.05$. C, Maximum force-generating capabilities. Fibers (n=9 to 11) were prepared from 3 isolated hearts of each group. D, The NFAT–luciferase reporter activity (RLU μg^{-1}) in the hearts at 5 months of age. n=4 in each group. *$P<0.05$. E, Western blot analyses in the hearts. Arrows indicate the calpain cleaved forms of talin and caspase-12. The graph indicates relative protein levels of cleaved talin or caspase-12 and ratio of cleaved forms to total proteins. n=4 in each group. *$P<0.05$.

tivity.[7] We examined myofilament Ca^{2+} sensitivity in mActin-Tg mice. The force-pCa relationship was shifted rightward in mActin-Tg mice compared with wild-type littermates (Figure 4A). The pCa value at half-maximal force generation (pCa50, an index of Ca^{2+} sensitivity) was significantly lower in mActin-Tg mice (Figure 4B), suggesting that skinned cardiac muscle fibers prepared from mActin-Tg mice show a decrease in Ca^{2+} sensitivity of force generation. The degree was the same between 2 and 10 months of age (Figure 4B), suggesting that the reduction in Ca^{2+} sensitivity is not a result of cardiac dysfunction. Despite the reduced Ca^{2+} sensitivity, there was no significant difference in maximum force-generating capabilities between wild-type littermates and mActin-Tg mice (Figure 4C). The decrease in myofilament Ca^{2+} sensitivity is expected to influence intracellular Ca^{2+} handling in cardiomyocytes of mActin-Tg mice. To clarify whether intracellular Ca^{2+} levels in cardiomyocytes are changed in mActin-Tg mice, we examined the activity of Ca^{2+}-dependent enzymes such as calcineurin and calpain. We generated double-transgenic mice by crossing mActin-Tg mice and the transgenic mice carrying a luciferase reporter driven by a cluster of NFAT binding sites, which is activated by calcineurin-dependent NFAT proteins.[15] The NFAT–luciferase reporter activity was higher in mActin-Tg mice than in wild-type littermates at 5 months of age (Table IV in the online-only Data Supplement and Figure 4D). Furthermore, the ratio of the calpain-induced cleaved forms of talin and caspase-12 to total proteins was significantly increased in mActin-Tg mice compared with wild-type littermates (Figure 4E). We next examined Ca^{2+} transients in cardiomyocytes using fluo-3AM (Figure IVA in the online-only Data Supplement). Although the time to peak amplitude of Ca^{2+} was significantly slower in mActin-Tg mice than in wild-type littermates (Figure IVB in the online-only Data Supplement), there was no significant difference in peak amplitude between wild-type littermates and mActin-Tg mice at 2 and 10 months of age (Figure IVC in the online-only Data Supplement). The expression levels of SERCA2a, but not Na^+/Ca^{2+} exchanger, were decreased in mActin-Tg mice (Figure III in the online-only Data Supplement).

CaMKIIδ Is Activated in mActin-Tg Mice

It has been reported that among Ca^{2+}-dependent proteins, expression of CaMKIIδ is increased in human DCM hearts[24] and that overexpression of CaMKIIδ induces heart failure in mice.[25,26] We thus examined the expression and phosphorylation of CaMKIIδ and phosphorylation of its target protein, phospholamban (Thr17). The protein levels of total (both CaMKIIδB and CaMKIIδC) and phosphorylated CaMKIIδ and of phosphorylated phospholamban (Thr17) were increased in mActin-Tg mice compared with wild-type littermates (Figure 5A and Figure VA in the online-only Data Supplement), suggesting that CaMKIIδ is activated in mActin-Tg mice. The protein levels of phosphorylated phospholamban (Ser16), which is activated by protein kinase A, were also increased in mActin-Tg mice (Figure 5A).

Because it has been reported that the sympathetic nervous system is activated in failing hearts and that β-adrenergic

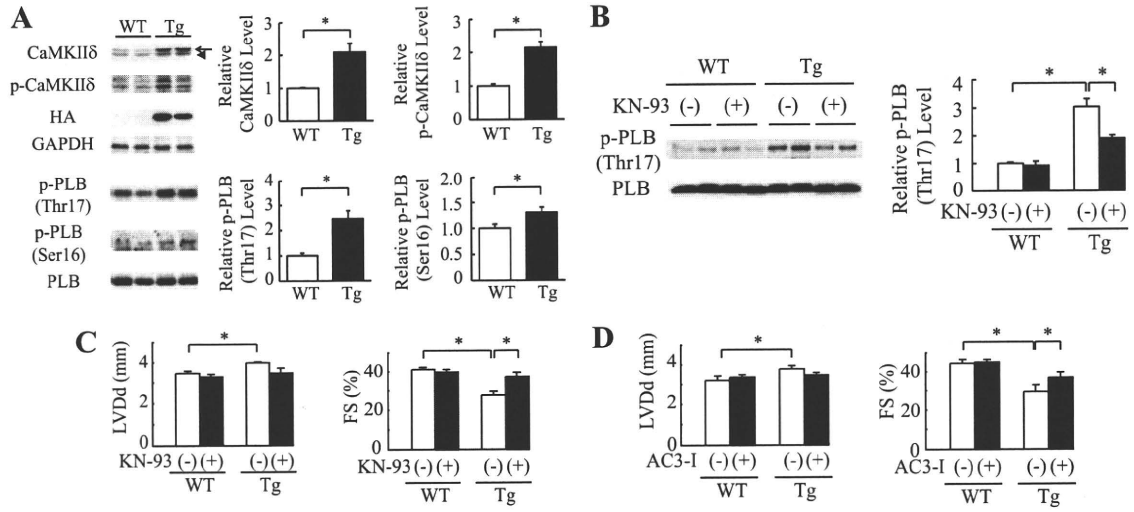

Figure 5. CaMKIIδ is activated in mActin-Tg mice. A, Western blot analyses in the hearts of wild-type littermates (WT) or mActin-Tg (Tg) mice at 5 months of age. The graph indicates relative protein levels of total and phosphorylated CaMKIIδ (p- CaMKIIδ) or phosphorylated phospholamban (p-PLB). Arrow and arrowhead indicate CaMKIIδB and CaMKIIδC, respectively. n=6 in each group. *$P<0.05$. B, Western blot analyses in the hearts at 5 months of age. The graph indicates relative protein levels of p-PLB (Thr17). n=4 in each group. *$P<0.05$. C and D, Echocardiographic analyses at 5 months of age. WT/KN-93(−), n=11; WT/KN-93(+), n=7; Tg/KN-93(−), n=8; Tg/KN-93(+), n=6; WT/AC3-I(−), n=8; WT/AC3-I(+), n=18; Tg/AC3-I(−), n=10; Tg/AC3-I(+), n=14. KN indicates KN-93; LVDd, left ventricular end-diastolic dimension; and FS, fractional shortening. *$P<0.05$.

receptor signal activates CaMKIIδ,[27] we treated mActin-Tg mice with the β-blocker bisoprolol to clarify the relationship between β-adrenergic receptor signal and activation of CaMKIIδ. The treatment with bisoprolol ameliorated cardiac dysfunction of mActin-Tg mice, and there was no significant difference in cardiac function between wild-type littermates and mActin Tg mice with bisoprolol treatment (Figure VB in the online-only Data Supplement). Furthermore, the increase in CaMKIIδ levels in mActin-Tg mice was prevented by bisoprolol treatment (Figure VC in the online-only Data Supplement), suggesting that the activation of CaMKIIδ in mActin-Tg mice might be due to activation of β-adrenergic receptor signaling.

To test whether activation of CaMKIIδ induces cardiac dysfunction, we first treated mActin-Tg mice with KN-93, a CaMKII inhibitor. Levels of both phosphorylated phospholamban (Thr17) and phospholamban (Ser16) were decreased by KN-93 treatment in mActin-Tg mice (Figure 5B and Figure VD in the online-only Data Supplement). Echocardiography revealed that KN-93 treatment prevented left ventricular dilatation and preserved cardiac function in mActin-Tg mice (Figure 5C). On the other hand, KN-92, an inactive derivative of KN-93, did not show any effects (Figure VE in the online-only Data Supplement). To confirm the role of CaMKIIδ in mActin-Tg mice, we crossed mActin-Tg mice and AC3-I mice, which expressed the CaMKII-inhibitory peptide AC3-I in the heart [mActin(+)/AC3-I(+)-DTg].[16] Echocardiography revealed that fractional shortening was better in mActin(+)/AC3-I(+)-DTg mice than in mActin(+)/AC3-I(−)-Tg mice (Figure 5D), suggesting that the activation of CaMKIIδ in the DCM mouse model induces left ventricular dilatation and contractile dysfunction.

We next examined the relation between CaMKIIδ activation and p53. The increase in p53 was attenuated by treatment with KN-93 or overexpression of AC3-I (Figure 6A and Figure VIA in the online-only Data Supplement). Furthermore, KN-93 treatment inhibited the increase in Bax expression and TUNEL-positive cardiomyocytes (Figure 6A and 6B). It has been reported that CaMKIIδC, but not CaMKIIδB, induces cardiomyocyte death.[27–29] To clarify the mechanism of how CaMKIIδ increases protein levels of p53 and which

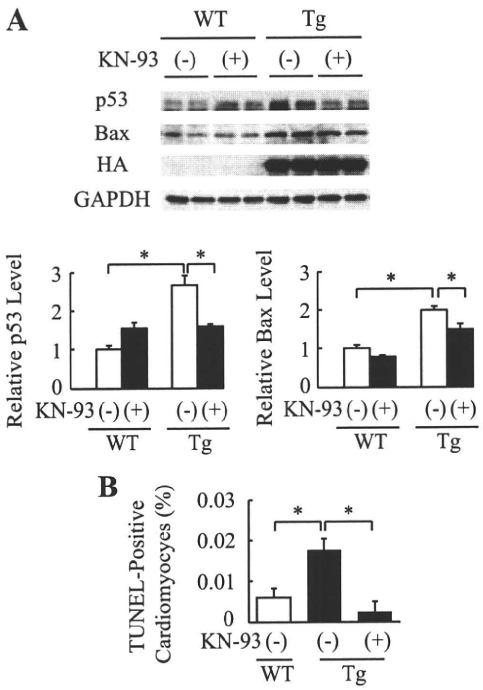

Figure 6. CaMKIIδ regulates expression of p53 in cardiomyocytes. A, Western blot analyses in the hearts of wild-type littermates (WT) or mActin-Tg (Tg) mice. The graph indicates relative protein levels of p53 or Bax. n=4 in each group. *$P<0.05$. B, Quantitative analyses of TUNEL-positive cardiomyocytes. n=5 in each group. *$P<0.05$.